GRS - 415

Performance Assessment of Sealing Systems

Conceptual and integrated modelling of plugs and seals

GRS - 415

**Gesellschaft für Anlagen-
und Reaktorsicherheit
(GRS) gGmbH**

Performance Assessment of Sealing Systems

Conceptual and integrated modelling of plugs and seals

André Rübel
Dieter Buhmann
Jonathan Kindlein
Thomas Lauke

August 2016

Abstract

The long-time isolation of radionuclides from the biosphere is the goal of the storage of radioactive waste in deep geological repositories. For repositories in rock salt, this goal is achieved on the one hand by the impermeable undisturbed part of the salt host rock formation and on the other hand by crushed salt, which is used to backfill the mine openings in the emplacement areas and galleries created during the construction of the repository. The crushed salt backfill is compacted over time and achieves a sufficiently high hydraulic resistance to avoid inflow of brines into the emplacement areas of the repository in the long-term. Plugs and seals must additionally provide their sealing function during the early post closure phase, until the compaction of the backfill is adequate and the permeability of the backfill is sufficiently low.

To assess the future development of the waste repository, an adequate knowledge of the material behaviour is necessary and related mathematical models must be developed to be able to perform predictions on the long-term safety of the repository. An integrated performance assessment model was formulated that describes the long-term behaviour of a sealing built from salt concrete. The average permeability of the sealing changes with time after its emplacement from various processes of which two were regarded in a constitutive model: first, the healing of the EDZ in the host rock around the sealing, and second, the corrosion of the salt concrete material resulting from brine attack. Empirical parameter model functions were defined for both processes to reflect the actual behaviour. The mathematical model was implemented in the integrated performance assessment model LOPOS which is used by GRS as near-field model for repositories in salt.

Deterministic and probabilistic calculations were performed with realistic parameters showing how the permeability of the sealing decreases during the first 2 000 years due to the healing of the EDZ. Between 2 000 and 3 000 years, the calculated curves show a minimum permeability. After this time, the permeability increases again due to the progressing cement corrosion. A set of parameter variations and a probabilistic assessment was performed to determine the influence of parameter uncertainty. The example calculations show that the constitutive model is suitable to be used for future integrated performance assessment.

Zusammenfassung

Der Endlagerung von radioaktiven Abfällen in tiefen geologischen Formationen mit hohem Einschlussvermögen ist der angestrebte Weg, die in den Abfällen enthaltenen Radionuklide von der Biosphäre fern zu halten. Bei Endlagern im Salz wird der Einschluss durch den ungestörten Teil der undurchlässigen Wirtsformation aus Salzgestein erreicht, in Verbindung mit Verschlussmaßnahmen in den Zugangsstrecken und Schächten, die bei der Erstellung des Endlagers aufgefahren werden. Die dauerhaften Verschlussmaßnahmen bestehen für ein Endlager im Salz in der Verfüllung aller offener Hohlräume mit Salzgrus, der mit der Zeit durch die Konvergenz des Salzgesteins eine ausreichend geringe Permeabilität erreicht. Zusätzliche Verschlussbauwerke müssen den Verschluss des Endlagers innerhalb der ersten einige tausend Jahre sicherstellen, bis der Salzgrus ausreichend kompaktiert ist.

Für die Prognose der zukünftigen Entwicklung des Endlagersystem ist ein adäquates Wissen über das Verhalten der in den Verschlussbauwerken verwendeten Materialien notwendig und es müssen entsprechende mathematische Modelle entwickelt werden. Im Rahmen des durchgeführten Projekts wurden integrierte langzeitsicherheitsanalytische mathematische und numerische Modelle entwickelt, die die langfristige Entwicklung von Verschlussbauwerken aus Salzbeton beschreiben. Dabei wurden der Einfluss der Korrosion des Salzbetons auf Grund des Kontakts mit zutretenden Lösungen und die zeitliche Entwicklung der Auflockerungszone um das Verschlussbauwerk berücksichtigt. Das Modell wurde in das Rechenprogramm LOPOS der GRS integriert, welches zur Durchführung von Langzeitsicherheitsanalysen für Endlager im Salz verwendet wird.

Es wurde exemplarisch die Betrachtung eines generischen Verschlussbauwerks mit deterministischen und probabilistischen Rechnungen unter Verwendung von realistischen Parameterwerten durchgeführt. Diese zeigen, dass sich während der ersten 2 000 Jahren die Verschlusspermeabilität auf Grund der Verheilung der EDZ verringert. Nach 2 000 bis 3 000 Jahren erreicht die Permeabilität ein Minimum und steigt dann auf Grund der fortschreitenden Zementkorrosion wieder an. Parametervariationen und probabilistische Rechnungen wurden durchgeführt, um den Einfluss der Parameterunsicherheit zu untersuchen. Die durchgeführten Beispielrechnungen zeigen, dass das entwickelte Modell geeignet ist, um in zukünftigen langzeitsicherheitsanalytischen Rechnungen eingesetzt zu werden.

Table of contents

1   Introduction

This report presents the work performed by GRS as part of the European project DOPAS (Full scale Demonstration of Plugs and Seals) and the national German project PASS (Performance Assessment of Sealing Systems) under the tasks on "Conceptual models and simulation of relevant processes and their evaluation within individual sealing components" and "Development of conservative PA methodology and models for analysing the complete system". The work is related to the research and development on plugging and sealing for repositories in salt and is of fundamental importance for the salt concept. The concepts used for development and testing in the following are based on results obtained in the German research project Preliminary Safety Analysis for Gorleben[1] (VSG) and precedent research projects like /BUH 10/.

In rock salt, the long-time isolation of the radioactive waste from the biosphere is done by the salt. This is on the one hand the undisturbed part of the salt host rock formation and on the other hand the crushed salt, which is used to backfill the mine openings in the emplacement areas and galleries. The crushed salt backfill is compacted over time and achieves a sufficiently high hydraulic resistance to avoid entries of brines into the emplacement areas of the repository. Plugs and seals must provide their sealing function during the early post closure phase, until the compaction of the backfill is adequate and the permeability of the backfill is sufficiently low. At a certain stage, backfill and host rock both have a permeability in the same order of magnitude. Research during the VSG project shows that the process is finished after a few thousands of years, at most /MUE 12b/. The shaft seal is designed to keep its function until the next ice age, which is expected to occur in 50,000 years. After the ice age, hydro-geologic and topographic conditions change due to the glaciation and a prediction of the chemical composition of waters flowing in is of high uncertainty, which makes it impossible to design robust seals against those chemical conditions. During later times, after the next ice age, the main sealing function is achieved by the host rock and the compacted backfill /MUE 12a/.

The following two terms related to sealings are used in the German repository context: The first one is the definition of "seal" as given in the German Safety Requirements /BMU 10/: "*A seal refers both to the sealing of the emplacement zones by flush mount*

---

[1]   German: Vorläufige Sicherheitsanalyse für den Standort Gorleben

backfilling of selected galleries and underworkings, as well as to the sealing of the shafts in the repository mine. The seal includes all technical structures incorporated into the repository mine in order to safeguard the integrity of the isolating rock zone and protect against ionising radiation." And the second one is the definition of "sealing element" as given in the safety and assessment concept of the VSG /MOE 12/: „*Ein Dichtelement ist Bestandteil einer technischen Barriere. Es hat die Aufgabe, gegen das Eindringen/Austreten von Fluiden einerseits und den Transport von Radionukliden andererseits zu wirken.*"[2].

---

[2] Translation: A sealing element is part of a technical barrier. It has the function to hinder the flow of fluids and the transport of radionuclides.

2   Disposal concept

The Gorleben salt dome has been investigated as potential site for a repository for high-level waste since the end of the 1970s. A site-specific research project, the Preliminary Safety Analysis for Gorleben, has been conducted from July 2010 to March 2013 to sum up the results of the Gorleben investigation achieved so far, to update the concepts for e.g. emplacement, repository layout, sealing and performance assessment and to compile remaining open questions.

In this chapter, the repository concept used in the VSG is shortly summarized. It considers the disposal of the following waste types:

1. HLW: spent fuel and vitrified high level waste and

2. ILW: waste types that are directly related to the waste stream of the two high-level waste types listed for the first item i.e. vitrified effluents and sludges from reprocessing (CSD B) and compacted hull material and technological waste (CSD-C).

The repository layout and the sealing concept for the Gorleben site developed during the VSG project were adapted to the site-specific geologic boundary conditions, e.g. the chemical composition of groundwater or the geologic structure of the salt dome were considered in the shaft sealing layout. The adaptation of the sealing strategy and the assessment of the long-term sealing behaviour used in the following have been important topics in the research project and are presented in two reports /MUE 12a/, /MUE 12b/.

The absolute amount of the wastes to be disposed of in the future that fall into these two categories are fairly well known due to the phase out from nuclear energy in Germany. The inventories regarded in the VSG are given in /PEI 12/. As an option, the additional storage of waste types with negligible heat generation in a separate area in the repository wing with a distance between both wings of about 400 m was examined within the scope of the VSG. The waste types considered in this option were

3. wastes containing graphite, depleted Uranium tails and other, non-specified wastes.

The sealing concept of the repository mine which is summarized in chapter 3 is independent from the amounts of waste to be disposed of and is similar for both repository wings, with drift seals separating the emplacement area from the infrastructural area.

The following description of the disposal concept refers to the repository concepts developed within the scope of the VSG /BOL 11/, /BOL 12/. The emplacement fields for spent fuel and HLW are located in the north-eastern part of the repository. The entire layout of the repository is shown in figure 2.1. Two emplacement concepts are considered for the repository in a salt dome. These concepts are either drift disposal or vertical borehole emplacement of disposal containers (e.g. POLLUX casks and spent fuel canisters (BSK 3)) The emplacement of transport and storage casks (type CASTOR®) in horizontal boreholes was considered for comparison only. The following description focuses on the two emplacement concepts, i.e. drift disposal and borehole disposal.
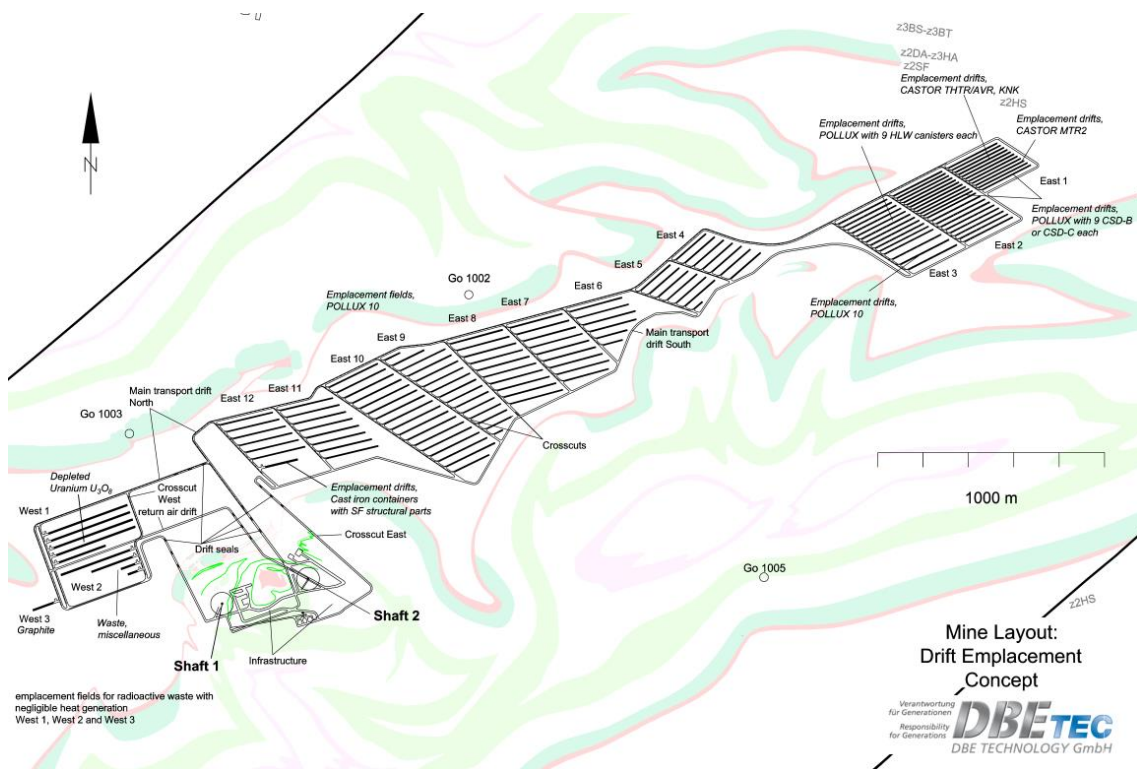

Fig. 2.1   Layout of the entire repository for the drift disposal concept /BOL 12/
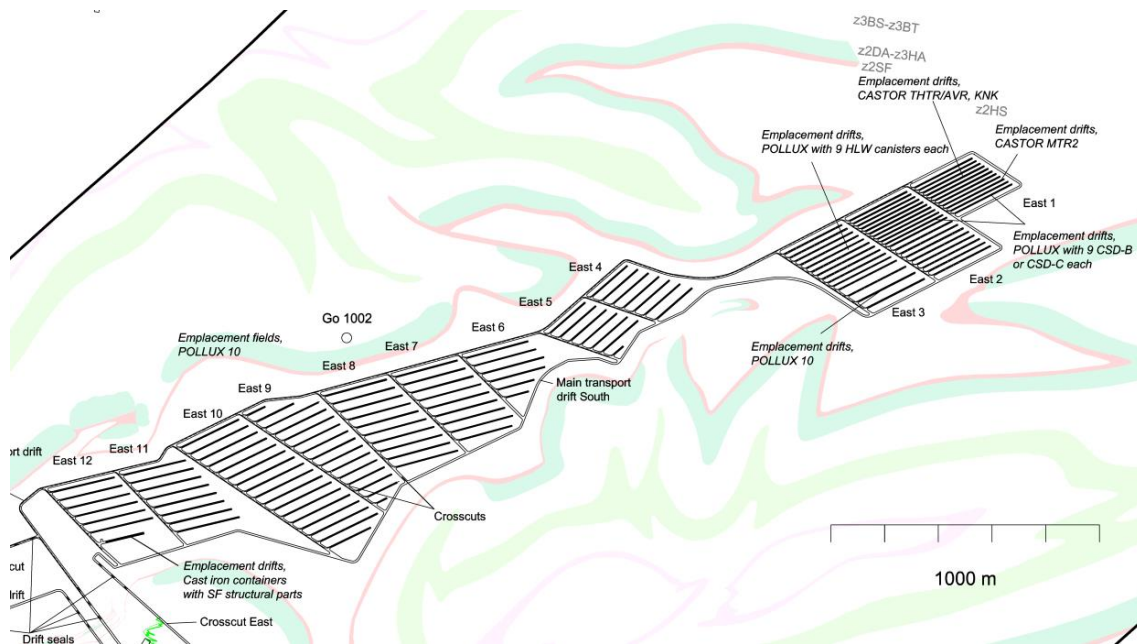
Drift disposal concept

Fig. 2.2   Layout of the north-eastern part of the repository for drift disposal /BOL 12/

The emplacement fields are tailored in such a way that they are completely embedded in the main salt (zsHS) of the salt dome. The repository layout took into account the known and expected geologic situation at the emplacement level (870 m below ground) of the salt dome.

Two main transport drifts are the northern and southern boundaries of the twelve emplacement fields (East 1 to East 12). Each emplacement field consists of a cross-cut and several parallel emplacement drifts in which the waste containers are emplaced on the floor. After the containers have been emplaced, the void spaces of the emplacement drifts are backfilled with dry crushed rock salt. There is no requirement to seal each single emplacement drift. Optionally, the emplacement field is sealed with a 10-m-long plug at both ends of the cross-cuts for operational reasons. There are no specified requirements for these plugs for the post-operational phase. The main transport drifts are backfilled with crushed salt as well, but with a water content of 0.6%wt, to accelerate the compaction process.

Drift seals are located close to the infrastructure area. Each drift seal consists of two 50-m-long sealing elements made of MgO-based concrete and three support elements. The total length of a drift seal is about 150 m. The infrastructure area is backfilled with

non-compactible serpentine gravel of high porosity to allow potential brines and gases to accumulate. The shafts are both backfilled and sealed over a length of nearly 600 m with a sequence of three sealing elements and multiple static abutments. A detailed description of the drift and shaft seals is given in /MUE 12b/ and is summarized in chapter 3.
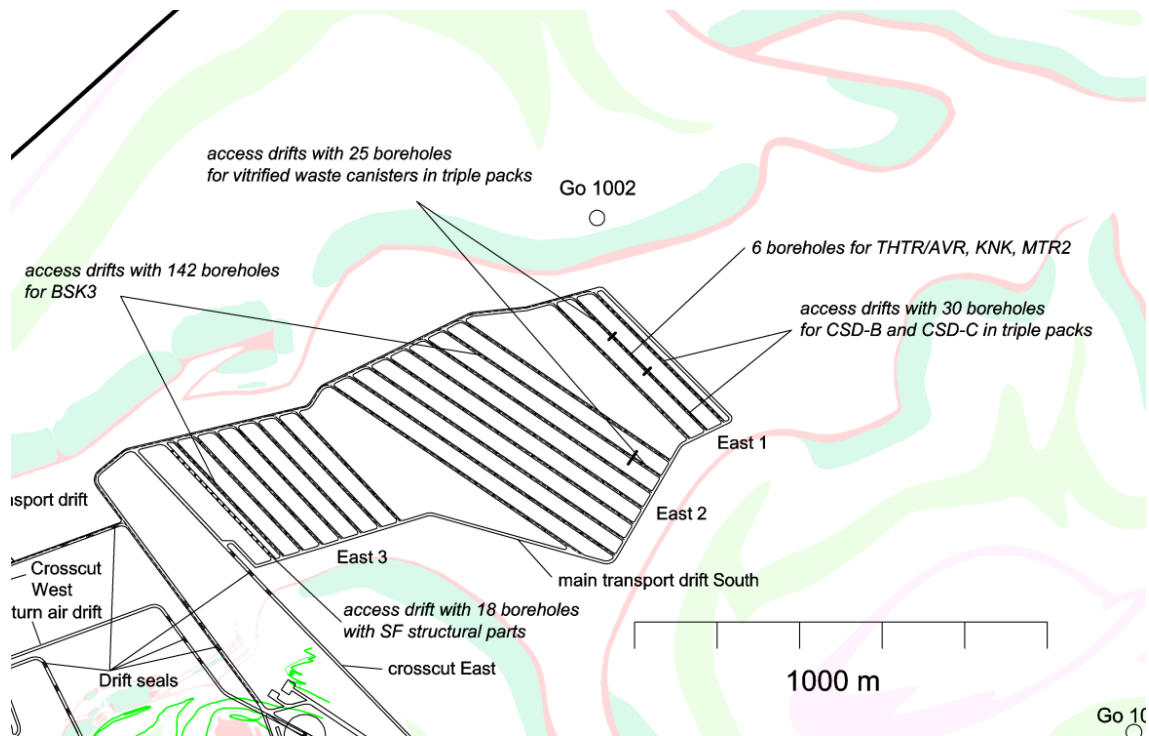
Borehole disposal concept

Fig. 2.3   Layout of the north-eastern part of the repository for borehole disposal /BOL 12/

For the borehole disposal concept, two main transport drifts are the northern and southern boundaries of the emplacement fields. The main transport drifts are intercon-nected by the access drifts. In each access drift, 7 to 15 vertical boreholes with a depth of up to 300 m are drilled into the host rock. The boreholes are supported by steel lin-ers to allow for the possibility to retrieve waste canisters during the operational phase as required by the regulations /BMU 10/. The void spaces between the steel liner and the containers are backfilled with quartz sand. After one borehole is filled, it will either be sealed with a steel lid or with a plug for operational reasons. There are no specified requirements for these plugs for the post-operational phase.

The backfilling and sealing of the drifts and shafts and the backfilling of the infrastructure area are comparable with the drift disposal concept. The locations and the layout of the drift and shaft seals are also the same.

Time schedule for emplacement

Considerations carried out in the VSG result in an operational period of the repository of around 100 years The plan for the operational sequence was developed as follows /BOL 12/:

1. The emplacement starts in the area most distant from the shaft (East1).

2. The void spaces around each container are backfilled with crushed salt immediately after emplacement.

3. After all emplacement drifts of an emplacement field are loaded, the connection gallery is backfilled and sealed at both ends with an MgO-based concrete plug of 10 m length.

4. The access drifts are backfilled with crushed salt.

5. The access drifts are sealed with a drift seal after emplacement is finished.

6. The infrastructure area is backfilled with gravel.

7. The shafts are sealed with shaft seals.

Steps 1 to 4 are successively performed during operation and steps 5 to 7 during closure of the mine. The time needed for the closure was estimated to five years. Therefore, according to this schedule, the construction of drift and shaft sealings start earliest in the next century.

3 Sealing concept

The following description refers to the repository concepts developed within the scope of the Preliminary Safety Analysis for Gorleben (VSG). There are two types of seals that are related to long-term safety: shaft seals and drift seals. There are two shaft seals, one in each shaft and four drift seals. The locations of the drift seals are shown in figure 3.3. Additionally, there are seals that are only relevant during the operational period of the repository. In case of borehole emplacement these are borehole seals on top of each emplacement borehole and in case of drift emplacement these are seals to isolate each emplacement field (see also description in chapter 2).
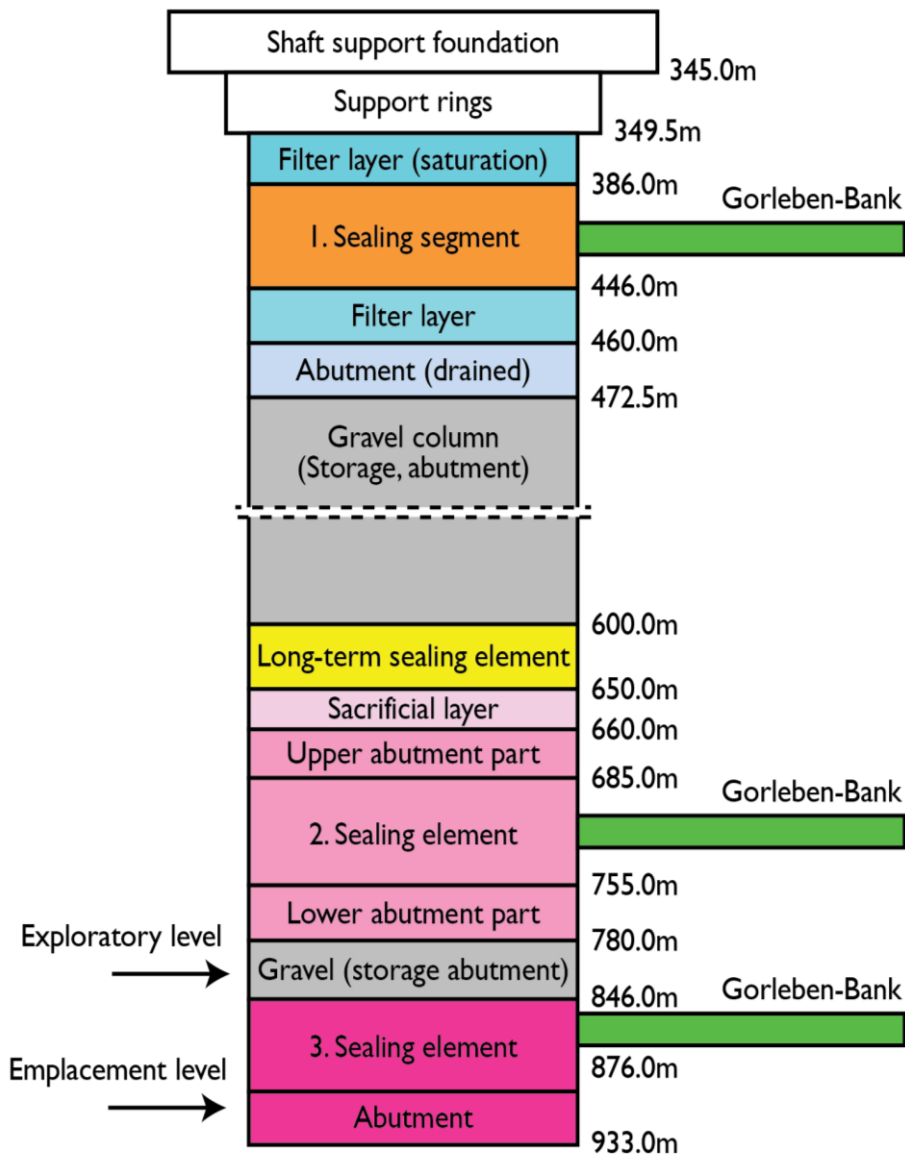

Fig. 3.1   Layout of the shaft seal after /MUE 12b/

The shaft seals each consist of three short-term sealing elements, one long-term sealing element (crushed salt) and multiple additional elements like abutments and reservoirs. The position of each element is related to the geologic structures like the Gorleben Bank and therefore slightly differs in both shafts. The layout of the shaft sealing for shaft 1 is shown in figure 3.1. The diameter of the shaft is 7.63 m. At the position of the sealing elements and abutments, the EDZ will be removed resulting in a larger diameter at these positions.

Short-term sealing materials must have a sufficiently low permeability that corresponds to the host rock permeability, must be stable against chemical and biological erosion, be stable against brines and stable in the long term. The realisations at the sealing locations have to consider the parallel arrangement of the seals, the contact area, and the residual part of the excavation damaged zone (EDZ).

Within the scope of the project VSG, the materials of the short-term sealings have been selected as follows: The first sealing element is made of bentonite. The material properties are similar to those of the salt clay at the top of the salt rock. It has a high cation exchange capacity. The swelling pressure of the bentonite allows the closure of the EDZ in low depths with only low rock pressure. This makes it suitable for the use in the upper short-term sealing element. The second sealing element is made of salt concrete. Salt concrete is stable against the expected brines at this place and creates diversity to the bentonite. Directly above the disposal level, a third sealing made of sorel concrete is located. The sorel concrete consists of magnesium oxide as adhesive cement and crushed salt as aggregate. In the lower part of the shaft, potash salt of the surrounding rock possibly changes the composition of the brines. Compared to salt concrete, sorel concrete is chemically stable against Mg-rich brines. Both types of concrete exhibit low permeabilities, and the convergence of the surrounding salt rock closes the EDZ.

The three sealing elements are designed as short-term seals. They are designed to maintain their functionality until the compaction of the backfill in the mine galleries is finished. In addition, there is a long-term sealing element in the shaft made of crushed salt. It is located between both concrete sealing elements. This salt layer compacts and reaches a permeability that is ultimately similar to the permeability of the host rock. /MUE 12a/.
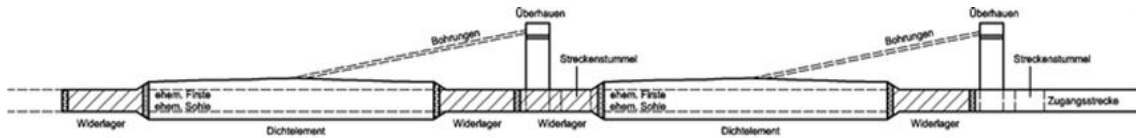
Fig. 3.2   Layout of the drift seal (side view) /MUE 12b/

The layout of the drift seals is shown in figure 3.2. The drift seals are not subject of investigation in DOPAS. Each drift seal consists of two sealing elements (Dichtelement, D), each 50 m in length and four abutments (Widerlager, WL), each 15 m in length. The sealing elements and abutments are both made of salt concrete. The main difference is that the EDZ is removed in the area of the sealing elements shortly before the construction of the sealing. The position of the drift seals is shown in figure 3.3.
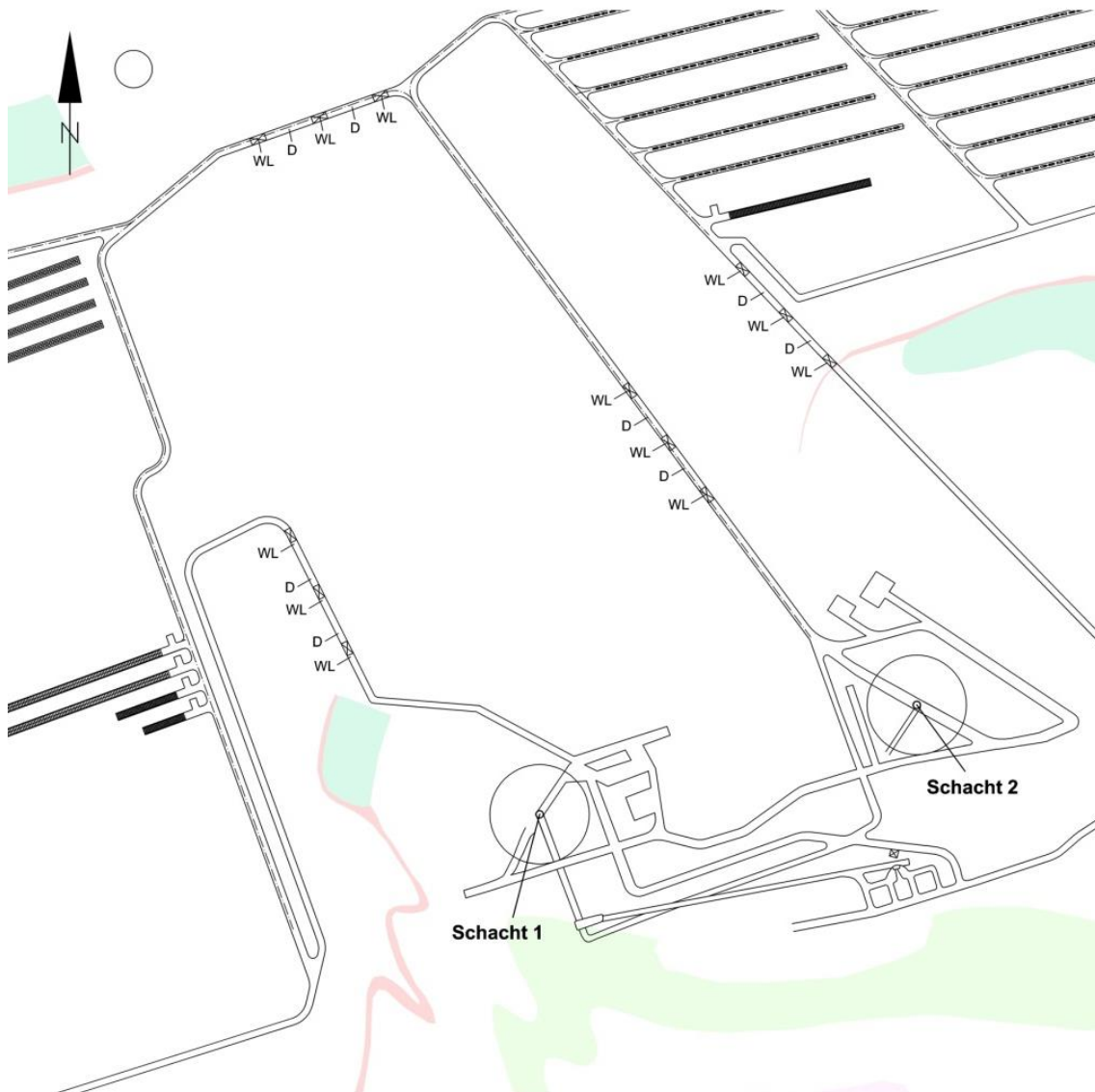

Fig. 3.3   Position of the drift seals /BOL 12/

13

The design of the shaft sealings in the VSG was developed in two steps, i.e. within one assessment loop. Performance assessment and process level modelling performed in the first step /MUE 12a/ were used to fix the final layout of the seals in the second step /MUE 12b/.

Three types of performance assessments have been performed for the first layout of the shaft seals which are geochemical, geomechanical and hydraulic assessments. A fully coupled performance assessment has not been conducted. The performance assessments tested the compatibility of the planned sealing system with the geologic and hydrological boundary conditions and the compliance with requirements from the safety concept /MOE 12/.

The geochemical process modelling of the sealing development considered dissolution and precipitation processes in the shaft sealing elements due to inflow of brines from the overburden, simulating the change of the solution composition on its path through the whole sealing system. The geomechanical process modelling considered mechanical loads on the sealing elements arising from rock pressure and hydraulic pressure to show that no fractures are created. Finally, the hydraulic assessments determined the amount of water flow through the sealing system to assess whether the permeability of the sealing system meets its requirement as safety function, which is to avoid contact of the waste with external waters. The performance assessments resulted in design changes of the sealing system into the final layout.

Uncertainties exist regarding the chemical composition of the groundwater at the shaft top. Probable future solution compositions were taken into consideration in the performance assessments. Future glaciation may influence the overburden geology and the groundwater composition in an unpredictable way. Therefore, no prediction was made for the state of the shaft seal for times later than 50.000 years from now.

The performance assessments of the future evolution of the shaft seal regarded all probable boundary conditions. To take remaining uncertainties into account, a less probable scenario of a failure of the shaft seal was created in the scenario development /BEU 12/ and considered in the long-term safety assessment for the VSG.

4   Integrated safety assessment code LOPOS

The integrated safety assessment code LOPOS (Loop structures in repositories) has been developed by GRS to simulate the one-dimensional, single-phase transport processes in the repository mine of a nuclear waste repository in salt /HIR 99/ and is one module of the code package RepoTREND (Transport and Retention of Non-decaying and Decaying contaminants in final Repositories) /REI 16/. A simulation includes the calculation of the inflow of brine from the overburden, through the mine to the emplaced waste, the mobilisation of the radionuclides from the waste matrix and the transport of the radionuclides through the repository mine up to the shaft top.

For modelling the transport in the repository mine, the mine is broken down into segments, each representing parts of the mine. These segments are linked in all six directions in space to ring-shaped paths finally representing any potential structure of a repository mine. In each of the segments the relevant processes like convergence of the salt host rock, reduction of void spaces and compaction of the backfill are simulated. Different segment types exist for open or backfilled spaces, drift, seals, shafts, emplacement locations and more to represent the different processes that have to be accounted for.

The fluid pressure, brine flow and radionuclide transport are calculated simultaneously by a non-linear balance equation for all segments on the basis of the equation of continuity. In porous media like backfilled drifts, a flow according to the Darcy law is assumed, while in open spaces a flow according to the equation by Hagen-Poiseuille is modelled.

The radionuclide transport between the different segments is simulated by the transport equation according to the method of finite elements with variable time stepping. As transport mechanisms advection, dispersion and diffusion and if applicable convection are taken into account. The discretisation of time is controlled by stability criteria of the equation solver.

The LOPOS code has been used for the safety assessments in the licensing procedure for the radioactive waste repository Morsleben (ERAM) for low and intermediate-level waste /BEC 09/, for simulations for the Asse mine /GRS 06/ and in the preliminary safety analysis for Gorleben (VSG) for the dimensioning of the seals /MUE 12b/. The LOPOS code was further used in several code benchmarks like in /BEC 02/ and in

/BOE 00/. In all comparisons the LOPOS code yielded good agreement with other codes used. Additionally LOPOS was verified using analytical solutions for selected cases yielding good results /HIR 99/.

5   Sealing model for integrated assessment

The detail of the representation of sealings in integrated performance assessments differs in the different national programmes. The long-term safety assessments for high-level waste in salt in Germany so far used approaches regarding the sealings as quasi homogenous elements. In this approach, the fluid flow through sealings is calculated by using an averaged permeability value over the whole cross-section of the sealing including a potential Excavation Disturbed Zone (EDZ). The permeability value is constant in time and conservative values are used to regard for special process like the EDZ or material alterations with time. More severe changes in permeability are taken into account by changing the permeability stepwise in time. This approach has also been used in the simulations for the VSG /LAR 13/. This chapter describes a mathematical model to overcome the limitations of the use of averaged permeabilities in integrated safety assessment and by this reduce conservatisms in the simulations.
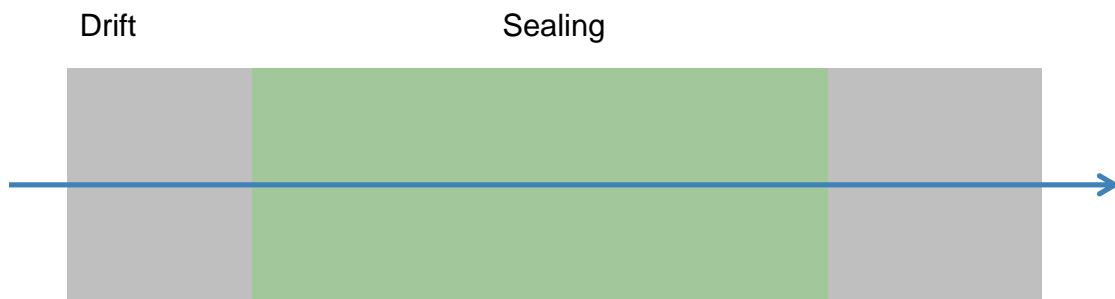
Drift   Sealing

Fig. 5.1   Homogenous sealing in integrated model[3]

According to Darcy's Law, the fluid flow j through a porous media is directly proportional to the gradient of the pressure p. The proportionality constant is the intrinsic permeability k.

$$j = \frac{A}{\mu} k \nabla p \tag{5.1}$$

---

[3] Although shaft sealing elements are regarded in the DOPAS project, the figures show drift sealings because of the better graphical layout. This however does not affect any of the considerations.

with

A flow area of the sealing,

μ dynamic viscosity of the fluid.

Two effects are to be considered in more detail in DOPAS, making the permeability a function of time t. The first one is the existence of an EDZ. The EDZ develops around excavations during the construction of the mine due to stress release. Most of the EDZ around sealing locations is removed by means of mining technique before sealing construction. However, part of the EDZ often cannot be removed or is quickly redeveloping during the time between EDZ removal and sealing construction. This disturbed zone around the drift section where the sealing is constructed has an increased permeability and extends up to several tens of centimetres into the rock.

The second process to be considered is the degradation of the sealing material by corroding fluids flowing through the sealing. In most cases, the sealing material is not in chemical equilibrium with the brine streaming in. This is the case, for instance, when MgCl-based concrete material is used for a sealing which is flown through by a sodium chlorine brine (or a NaCl-based concrete material which is streamed by a magnesium chlorine solution) resulting in a dissolution of minerals and precipitation of others. The permeability of the corroded material is typically higher than the initially used material. Due to the low permeability of the sealing, the corrosion process occurs within a sharp corrosion front slowly progressing through the sealing.

For the following model, the hydraulic resistance R of a sealing of length L is defined by

$$R = \frac{\mu L}{Ak} \tag{5.2}$$

This resistance can be used to calculate the effective sealing permeability for a sealing divided in different regions with different permeabilities using the well-known laws for series and parallel connection of resistances.
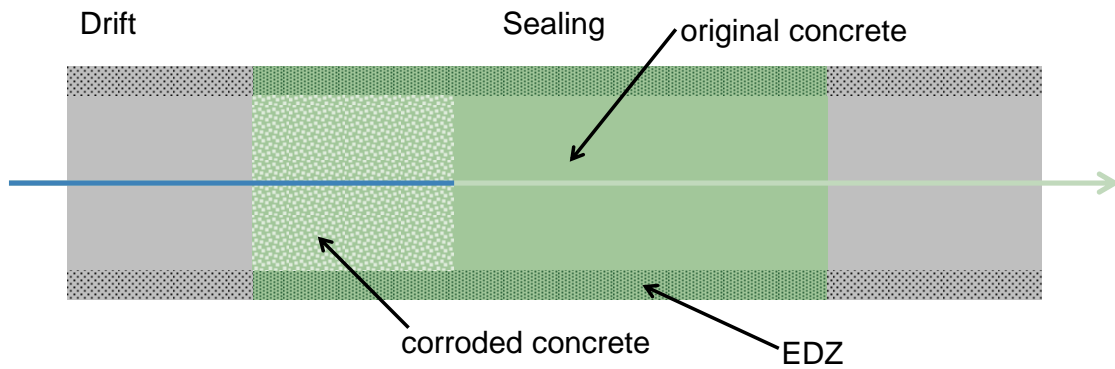
Fig. 5.2   Compartments of the sealing

Subsequently, the sealing is divided into three spatial separated compartments:

(i)   original concrete material,

(ii)   corroded concrete material and

(iii)   an EDZ.

The total resistance of the sealing can be calculated at each point in time from the fractional resistances of the individual compartments. It has to be noted, however, that due to the dependence of the resistance from the viscosity of the fluid, the resistance of a compartment might change over time just due to changes in fluid composition.
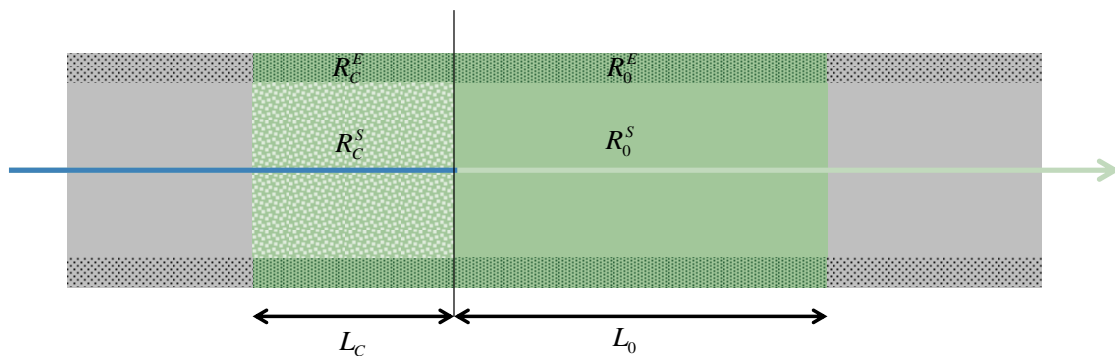

Fig. 5.3   Resistances of the sealing compartments

For each point in time, each of the compartments is characterized by a porosity ϕ, a density ρ, a brine viscosity μ and a permeability k. A lower index C denotes for the corroded region, while the lower index 0 denotes for the region still unaffected by corrosion. The upper index S refers to the sealing material, while the upper index E refers to the EDZ properties.

The total resistance of the entire sealing can be calculated from

$$R = R_C + R_0 = \frac{R_C^E R_C^S}{R_C^E + R_C^S} + \frac{R_0^E R_0^S}{R_0^E + R_0^S} = \frac{R_C^E R_C^S \left(R_0^E + R_0^S \right) + R_0^E R_0^S \left(R_C^E + R_C^S \right)}{\left(R_C^E + R_C^S \right) \cdot \left(R_0^E + R_0^S \right)} \qquad (5.3)$$

with

$$R_0^S = \frac{\mu_C L_0}{A^S k_0^S}, \quad R_0^E = \frac{\mu_C L_0}{A^E k_0^E}, \quad R_C^S = \frac{\mu_0 L_C}{A^S k_C^S}, \quad R_C^E = \frac{\mu_0 L_C}{A^E k_C^E} . \qquad (5.4)$$

6   EDZ evolution

Excavation disturbed zones (EDZs) in rock salt develop in the vicinity of cavities during and after excavation. The highly inhomogeneous stress state around a cavity leads to dilatancy, i.e., an inelastic increase in volume (and thus pore space) by microfracturing, and thus to a potential increase in permeability. The hydraulic properties of rock salt are significantly altered in the EDZ, an increase of permeability up to more than four orders of magnitude has been observed.

The hydraulic behaviour of the EDZ in rock salt has been investigated in the frame of various projects like the BAMBUS II project within the 5th EU-framework programme /BEH 04/. Conventional packer tests as well as investigations involving new developed permeability testing arrangements and geoelectrics were performed at different test areas in the Asse salt mine (Germany) to assess the extent and characteristics of the EDZ depending on excavation dimensions and stress state. For interpretation of the results, the measured permeabilities were related to the respective stress state of the rock which was concluded from finite element modelling.

In the context of waste repositories, the hydraulic behaviour of the EDZ is especially important around sealing structures to isolate disposal fields. It is, however, reckoned that dilatancy reduces and the EDZ heals when the stresses return to a more or less isotropic state after emplacing a supporting structure like the sealing.

The temporal evolution of the EDZ-permeability during the progression towards a homogenous stress state and the healing of the EDZ is to be described by a function

$$k_{EDZ} = f(t) \tag{6.1}$$

from existing experimental or process level modelling work. Since no admitted function is currently available describing the actual process, empirical parameter functions are used that are fitted to process level model results which are again using experimental data.

The computer code CODE_BRIGHT developed by the Technical University of Barcelona (UPC) is used by GRS for the analysis of coupled thermo-hydro-mechanical (THM) phenomena in geologic media. The development of CODE_BRIGHT started in the 1990's for the purpose of modelling the response of saline materials in the context of

underground nuclear waste disposal. The initial capabilities were soon extended to a wider range of geologic and technical materials and, in particular, unsaturated soils. A constitutive model for rock salt and crushed salt was implemented that contains both time-independent deformation as well as viscous material behaviour. Total deformation rate is calculated as the sum of contributions from the different deformation mechanisms /CZA 12/:

    (i)   Elastic deformation behaviour (M),

    (ii)   Viscoplastic coupled deformation behaviour (TM): loosening and recompaction of rock salt as well as grain re-organization of crushed salt,

    (iii)   Dislocation creep (TM),

    (iv)   Coupled viscous deformation behaviour (THMC): only used for crushed salt.

The suchlike extended CODE_BRIGHT model was used to simulate the temporal evolution of the EDZ porosity around salt concrete sealing elements for the Gorleben site (see figure 3.1, second and third sealing element). The results of these simulations are presented in figure 6.1. The temporal evolution of the EDZ porosity is plotted for different observation points at the top, middle and the bottom of both sealing elements. The porosity reduces from initially around 0.5% down to about 0.3% with about 10.000 years and is generally lower for the sealing element located at greater depth.

For hydraulic modelling, the porosity values have to be converted into permeability values. In the past, different equations were derived in experiments and proposed for the relationship of the permeability of the EDZ as a function of porosity. Two of them are given in the following. The first model represents a cubic law of a Kozeny-type relationship:

$$k = k_0 \left(\frac{\phi}{\phi_0} \right)^3 \qquad\qquad (6.2)$$

In case of the modelled EDZ, the primary porosity ϕ_0 is equal to 0.003 (figure 6.1) and the primary permeability k_0 is equal to $5 \cdot 10^{-20}$ m^2 (figure 6.2). Both values represent the salt rock properties of the undisturbed rock before the evolution of the EDZ.

The second model is an interpretation of permeability as a function of microfractures which are characterized by an aperture b_0 and a constant spacing s. This model is described in more detail in /OLI 08/. In this model, it is assumed that the changes in aper-

ture can be calculated as a function of deformations. When dilatancy takes place, permeability increases. Compression below the initial aperture does not produce further decrease of permeability as it is assumed that the matrix permeability is constant. The function of Olivella is given by

$$k = k_0 + \frac{(b_0 + s \cdot (\phi - \phi_0))^3}{12 \cdot s} , \; b_0 = 5 \cdot 10^{-8} \text{ m}, \; s = 2 \cdot 10^{-4} \text{ m} \tag{6.3}$$

The two models specified above are both plotted together in figure 6.2. Two other functions proposed by DBETec and IfG are given on page 310 of /MUE 12b/ and plot in between the two curves shown.

Taking the porosity-curves for the five different observation points of the third sealing element from figure 6.1 and converting the porosity into a permeability using the function of Olivella, the permeability versus time functions depicted in figure 6.3 are received (blue curves). These curves are fitted by visual inspection using a sigmoidal fitting function:

$$k^E = k_\infty + k_0 e^{\left(-a \cdot t^b\right)} \tag{6.4}$$

With

t time in years,

k_0 initial permeability value at $t = t_0$; $k_0 = 4.5 \cdot 10^{-17}$ m^2,

k_∞ permeability value converging against after long times; $k_\infty = 1.61 \cdot 10^{-19}$ m^2 and

a, b curve shape fitting parameters; $a = 0.4$, $b = 0.35$[4].

---

[4] A least square optimization fit performed with the fitting engine of zunzun.com (function: Weibull 2D) by minimizing the absolute residual resulted in slightly different parameters: $k_0 = 3.58 \cdot 10^{-17}$ m^2, $k_\infty = 2.80 \cdot 10^{-19}$ m^2, $a = 0.4$, $b = 0.35$ which, however, by visual inspection doesn't fit as good as the values given above.

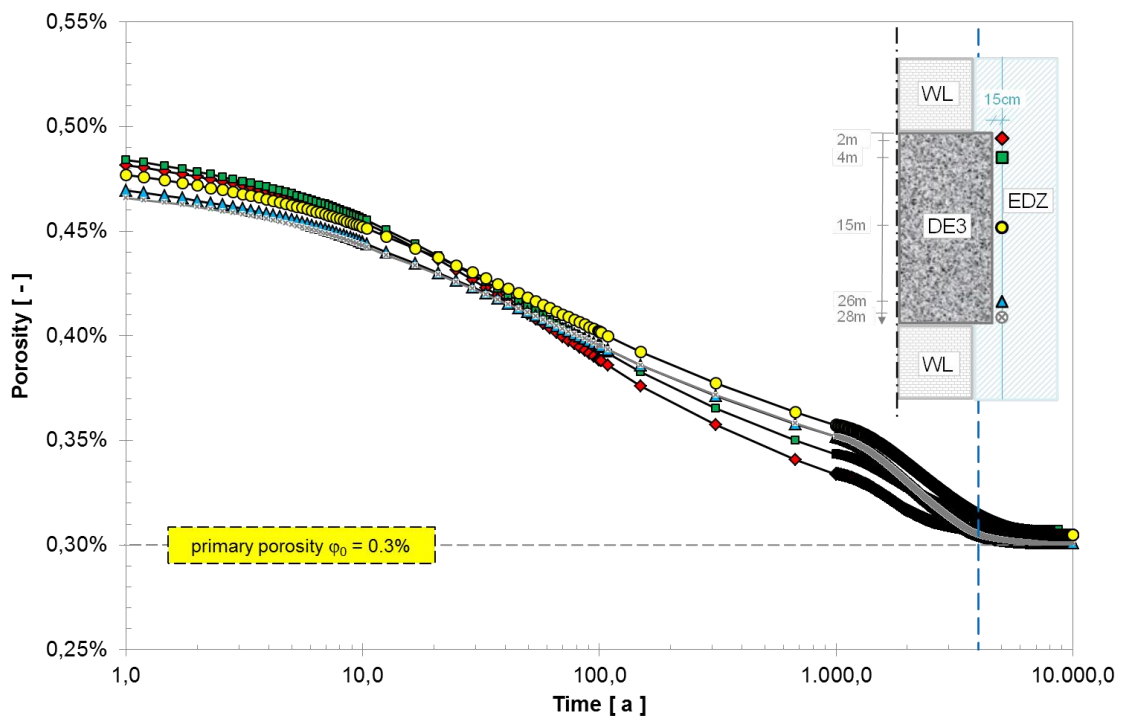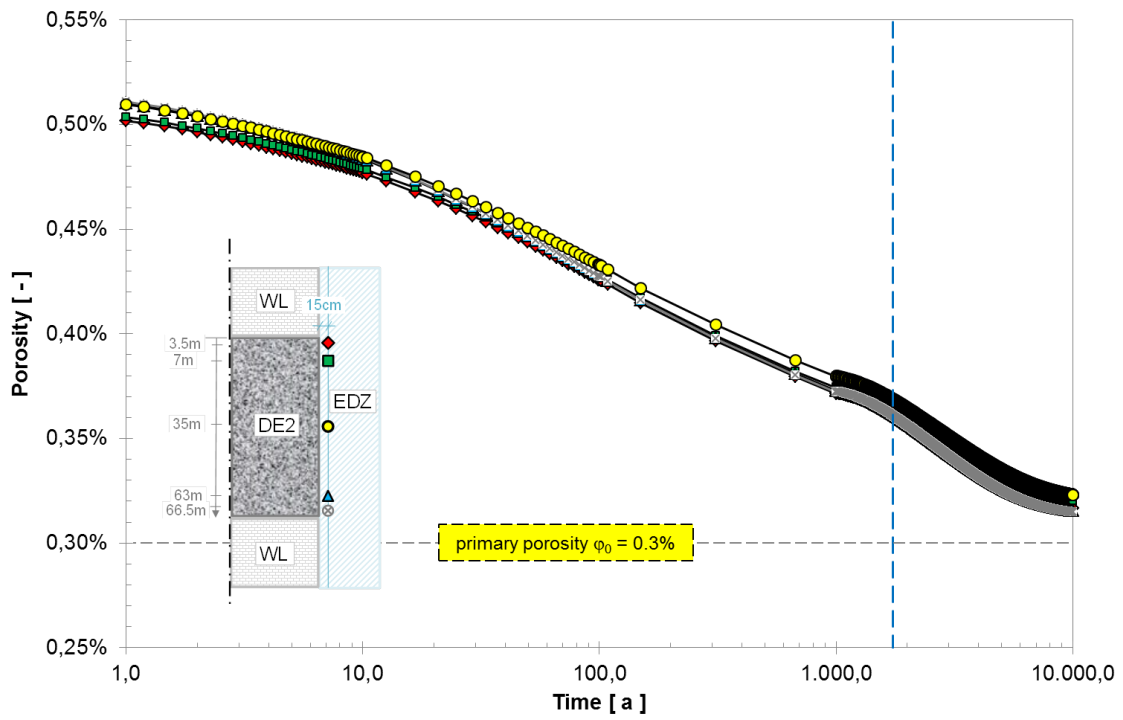**Fig. 6.1** Temporal evolution of porosity in the EDZ around second (upper picture) and third (lower picture) sealing elements /MUE 12b/
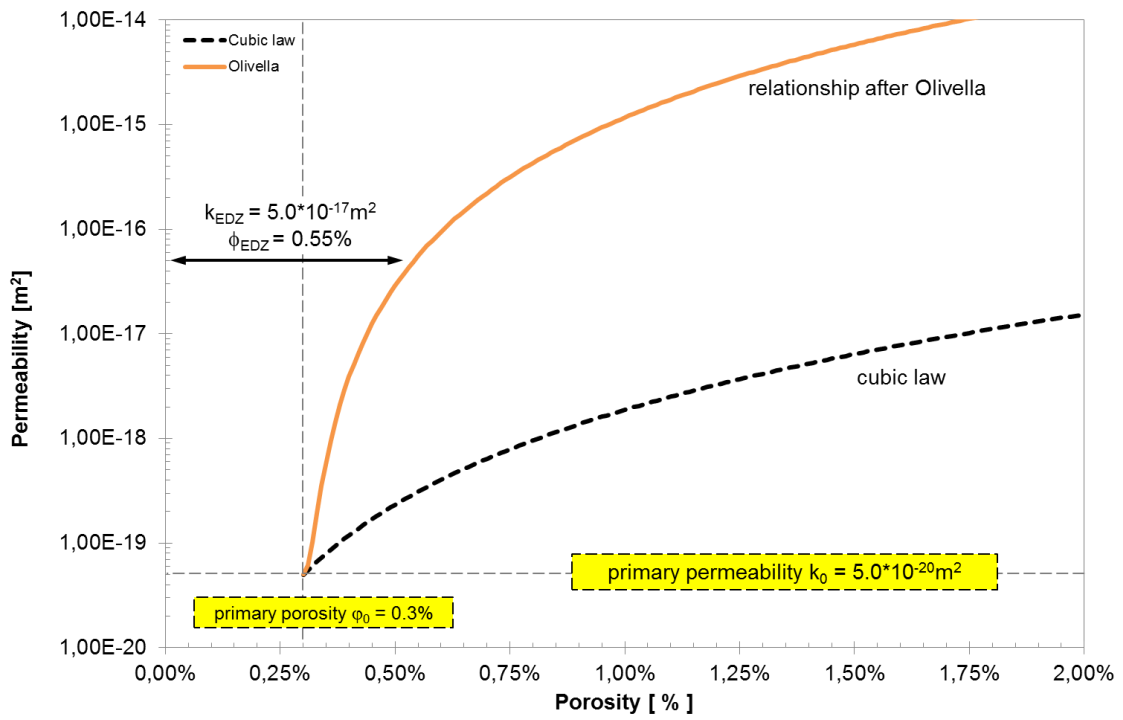
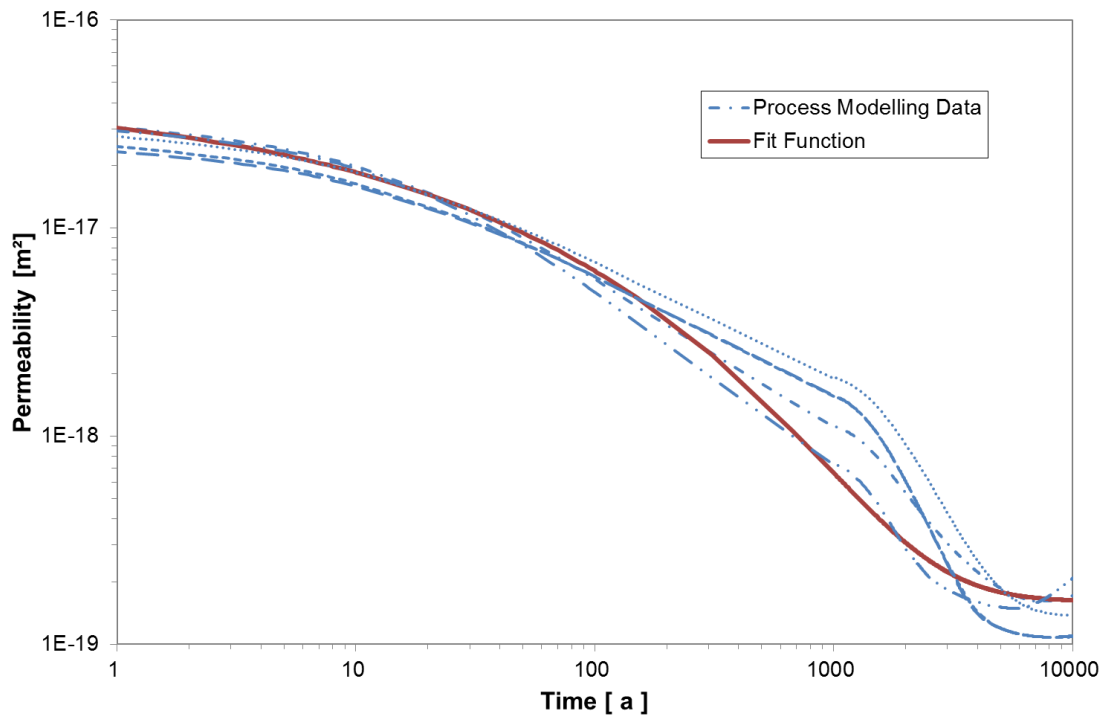**Fig. 6.2** Laws for porosity-permeability relationship in the EDZ

Fig. 6.3 Fit curve for the temporal evolution of EDZ permeability for sealing DE3

25

7   Corrosion of salt concrete

Salt concretes are considered as material for sealing elements like sealing element two and three of the concept regarded in the preliminary safety analysis for Gorleben (see figure 3.1). Crushed salt replaces sand and gravel as additive in salt concretes, which are used only in a salt environment. These materials consist mainly of cement, crushed salt and fly ash. In case of brine intrusion into the repository, the sealing elements made of salt concrete may be affected by significant changes regarding their mineralogy, their chemical composition as well as their hydraulic and mechanical properties. The changes are due to dissolution and precipitation reactions, inducing changes in brine composition and pH-value.

Cement corrosion processes of the cement matrix of concretes are divided phenomenological into leaching and swelling mechanisms. In leaching processes single solid phases will be dissolved leading to an increase of porosity and permeability. Swelling occurs if phases precipitate that have a higher volume than the starting phase assemblage. An overview of the corrosion processes is given in /BIC 68, HEW 98/. In case of a salt environment highly saline solutions can be expected. In contact to these solutions (NaCl rich and/or Mg-rich) degradation processes by combined magnesium and sulphate attack and CO_2 corrosion have to be taken into account.

Whereas the salt concrete will be corroded by IP21-solution, it is stable in NaCl solution. The opposite reaction behaviour was observed for MgO-based concrete. Laboratory tests as well as observations of technical structures show that the degradation of cement in magnesium sulphate solutions is characterised by a sharp corrosion front which penetrates slowly into the concrete. Beyond this front the cement maintains its original physical and chemical properties. Within the area where the intruding brine attacks the concrete, its physical strength and hydraulic properties are significantly changed by dissolution and swelling processes.

The extent of the concrete corrosion due to the reaction with saline solutions can be estimated by experiments and geochemical modelling and is to be considered in long-term safety assessment. The corrosion capacity $\kappa_{L,M}$ of a brine solution is defined by the mass of concrete M_c which is affected by corrosion by the volume V_B of brine /NOS 07/:

$$\kappa_{L,M} = \frac{M_C}{V_B} \tag{7.1}$$

Similarly, the corrosion capacity $\kappa_{L,V}$ can also be given by the grain volume of concrete V_{Cgrain} which is corroded by the volume V_B of brine

$$\kappa_{L,V} = \frac{V_{Cgrain}}{V_B} = \kappa_{L,M} \frac{1-\phi}{\rho} \tag{7.2}$$

with

V_{Cgrain}	grain volume of the concrete = $V \cdot (1-\phi)$,
V	geometrical volume of the concrete
ϕ	porosity of the concrete
ρ	density of the concrete.

For the corrosion of salt concrete magnesium is needed to be present in the solution. From the combination of leaching experiments and geochemical modelling, the corrosion capacity of IP21-solution on a special salt concrete called M2 was determined to be $\kappa_{L,V}$ = 1.04 l/l /HER 05/. The Mg concentration decrease in solution has been taken as indicator for the corrosion capacity in this modelling. A higher maximum corrosion potential of 2.4 l/l could theoretically be defined by using the calculated total consumption of Mg from the solution and the appearance of tobermorite as a thermodynamically stable mineral phase as shown in figure 7.1.

In the Preliminary Safety Analysis for Gorleben (VSG) the corrosion capacity of the brines flowing into the shaft for the uppermost salt concrete sealing element was estimated to be $\kappa_{L,V}$ = 0.225 l/l /MUE 12a/. In this case the complete sequence of reactions between inflowing solution and the available materials was considered in PhreeqC and EQ3/6 simulations. This shows that in any case, the corrosion capacity has to be determined specifically for the site specific situation.
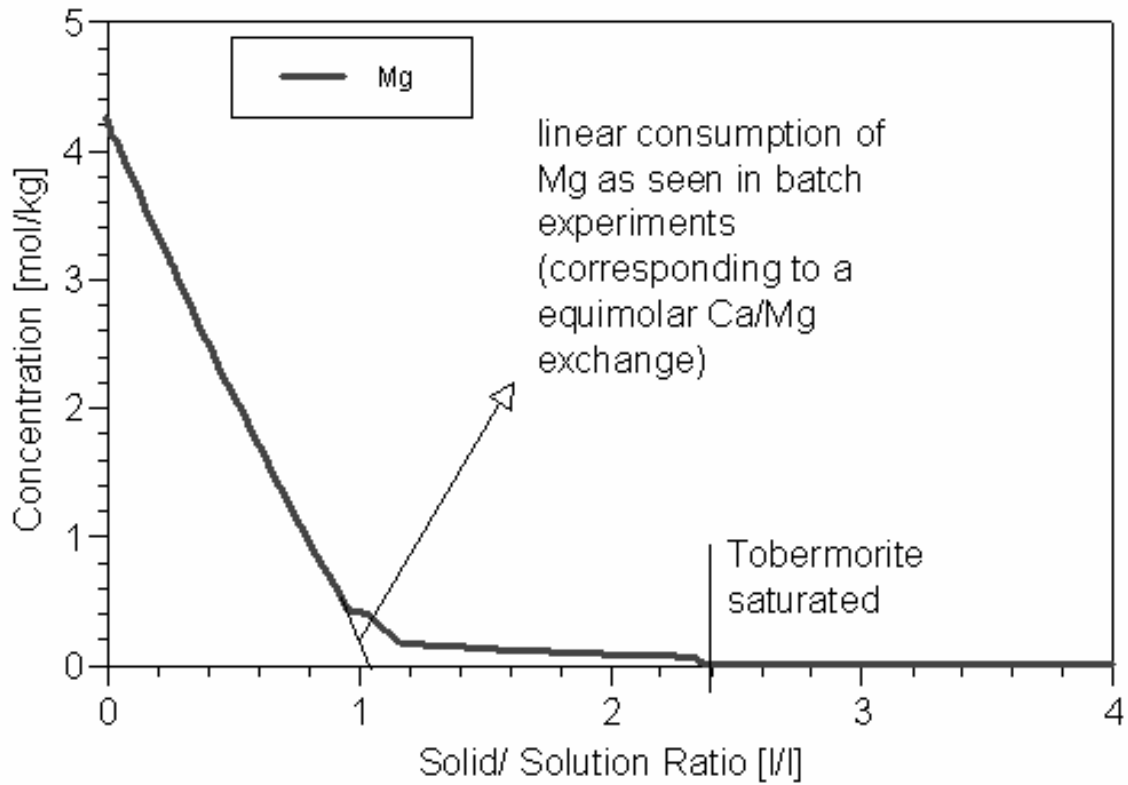
Fig. 7.1   EQ3/6 modelling of the reaction of salt concrete M2 with IP21 solution /HER 05/

The volume of brine V_{BC} which is needed to flow through the sealing until the corrosion front has reached the point L_C is given by the amount of brine needed to corrode the concrete plus the amount of brine needed to again fill the pore space with fresh unused brine:

$$V_{BC} = \frac{\left(1 - \phi_0^S\right)}{\kappa_{L,V}} A^S L_C + \phi_C^S A^S L_C \qquad (7.3)$$

with

A cross section of the sealing.

The resulting change in permeability is

$$k_C^S = 10^\varepsilon k_0^S , \qquad (7.4)$$

with the exponent ε giving the number of decades of permeability increase after corrosion of the concrete.

Assuming the EDZ is unaffected by the corrosion process, it is

$$\phi_C^E = \phi_0^E = \phi^E \text{ and } k_C^E = k_0^E = k^E \text{, but in general it is } \mu_C \neq \mu_0.$$

Assuming a homogenous sealing and neglecting changes in the brine viscosity and the existence of any EDZ, equations 5.3, 5.4, 7.3 and 7.4 yield a relative increase of the sealing permeability k_C^S / k_0^S as a function of brine flow through the sealing as exemplarily shown in figure 7.2. From this figure it is obvious that the permeability only slightly increases at the beginning and drastically increases towards the end if a constant brine flow rate is assumed.
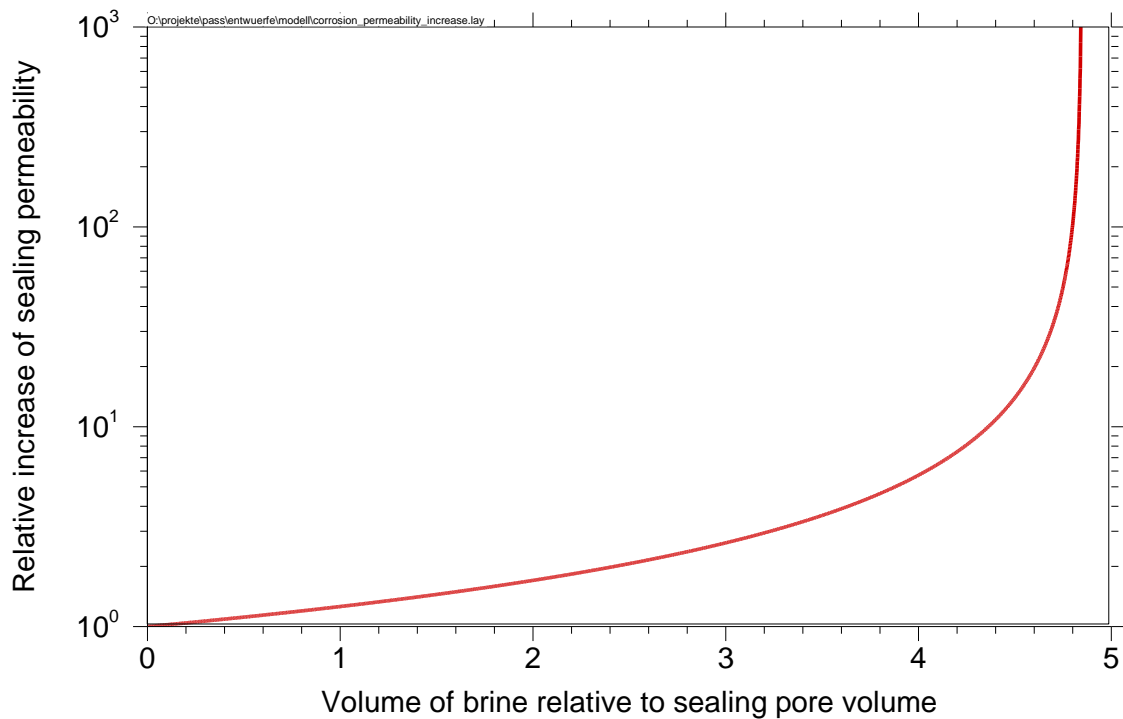
Fig. 7.2   Relative increase of sealing permeability as a function of brine volume flow

8   Illustrative example calculation

The influences on a sealing element of the two processes EDZ-closure and cement corrosion that have been discussed in the two preceding chapters are illustrated by an exemplary calculation in the following. The time dependent fluid flow is explicitly calculated by spreadsheet analysis according to the Darcy Law under the assumption of a constant pressure head at the sealing front face.

A sealing of 30 m in length is regarded with an initial permeability of the sealing core made from salt concrete material of $5 \cdot 10^{-19}$ m^2. The EDZ around the sealing radially extends 1 m into the rock and has an initial permeability of $4.5 \cdot 10^{-17}$ m^2. The EDZ behaviour with time and the cement behaviour under brine corrosion are considered in the way as discussed in the preceding chapters. The inflowing brine has a hydraulic pressure of 10 Pa, which is close to the fluid pressure expected on the emplacement level of the Gorleben mine. To simplify this example, a constant depth was assumed for the whole sealing length, what corresponds to a drift sealing rather than a shaft sealing. All parameters used for the example calculation are given in table 8.1.

Tab. 8.1   Example calculation parameters

Parameter		Value
Length of the sealing	[m]	30
Diameter of the sealing	[m]	7
Hydraulic pressure at sealing	[MPa]	10
Viscosity of brine μ	[Pa s]	$5.3 \cdot 10^{-3}$
Porosity of salt concrete material ϕ	[-]	0.2
Initial permeability of salt concrete material k_0^S	[m^2]	$5 \cdot 10^{-19}$
Permeability of corroded salt concrete material k_C^S	[m^2]	$1 \cdot 10^{-14}$
Corrosion capacity of the brine $\kappa_{L,V}$	[l/l]	1
Extension of the EDZ	[m]	1
EDZ initial permeability k_0	[m^2]	$4.5 \cdot 10^{-17}$
EDZ long-term permeability k_∞	[m^2]	$1.6 \cdot 10^{-19}$
EDZ fitting parameter a	[-]	0.4
EDZ fitting parameter b	[-]	0.35

The results of the simulation are shown in figures 8.1 and 8.2 which show the hydraulic resistance of the sealing and the volume flow through the sealing versus time. The black solid line denotes the resulting effective parameters across the entire cross section of the sealing, while the dashed lines show the same parameters, but distinguish between the concrete core of the sealing and the EDZ in the host rock around the sealing. It has to be noted that the first figure uses a logarithmic scale on the time axis while the second one uses a linear scale.

As is shown in figure 8.1, the hydraulic resistance of the sealing is dominated at the beginning by the comparatively low resistance of the EDZ. The EDZ is than recompacting with time and the resistance of the EDZ is increasing during the first 300 to 400 years by one order of magnitude. After about 500 years, the hydraulic resistance of the EDZ exceeds those of the sealing core, which dominates the resistance of the sealing thereafter. The hydraulic resistance of the sealing concrete core is nearly constant for nearly one thousand years. After one thousand years, the resistance is slowly decreasing due to the progressing corrosion process, but does not change more than a factor of two until about ten thousand years. After about 13 000 years, the hydraulic resistance is rapidly decreasing and reaches its minimum value after about 15 300 years. After this time, the cement sealing material is fully corroded.

The reciprocal behaviour is shown in figure 8.2 for the fluid flow through the sealing. The initially low hydraulic resistance of the EDZ results in a preferential fluid flow through the EDZ, exceeding the one in the sealing core by more than one order of magnitude. After two hundred years, the fluid flow is taking place mainly through the sealing. The flow rate first increases slowly until a drastic increase occurs around 15 000 years.

The integrated amount of brine inflow until the point in time of a sufficient high compaction of the crushed salt in the access drifts of the repository is the main quantitative performance requirement of the permeability of the shaft sealing. The permeability of the shaft seal is sufficiently low, if the amount of inflow does not completely fill the void spaces in the infrastructure area for the conditions expected in the reference scenario. The integrated amount of brine inflow is plotted in figure 8.3. The amount of brine until the complete corrosion of the seal is about 1 500 m^3. After this point in time, the amount of brine increases rather quickly to one million cubic meters of brine.
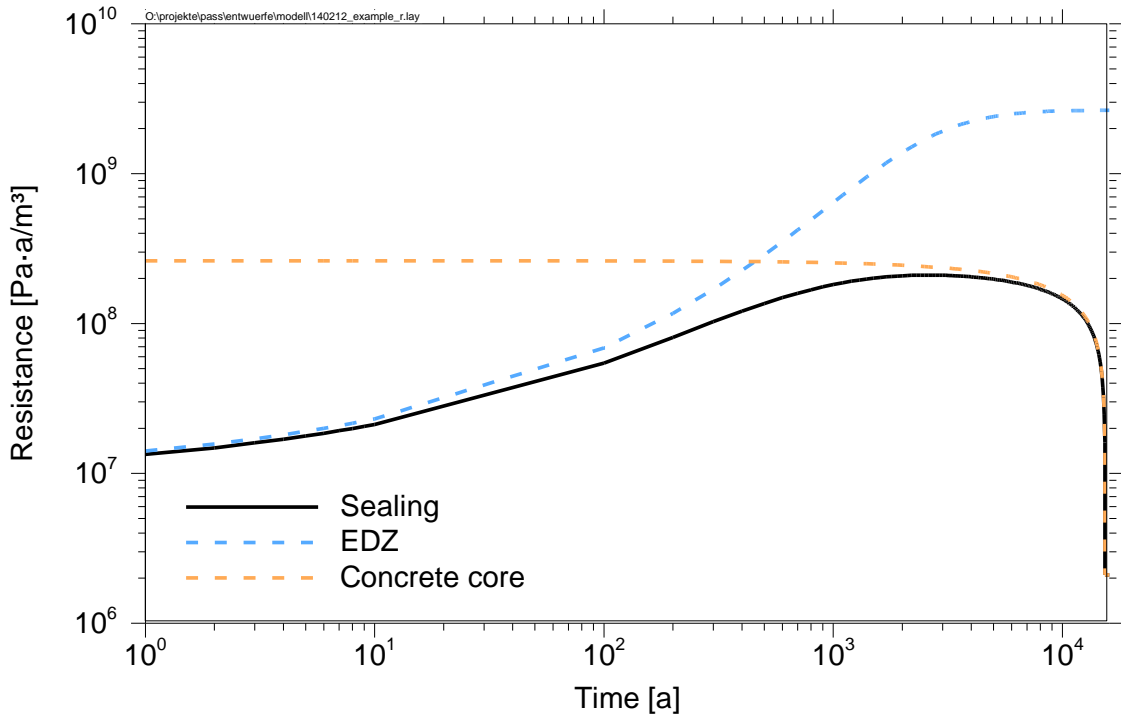
Fig. 8.1   Hydraulic resistance of a sealing, its concrete core and the EDZ around the sealing versus time
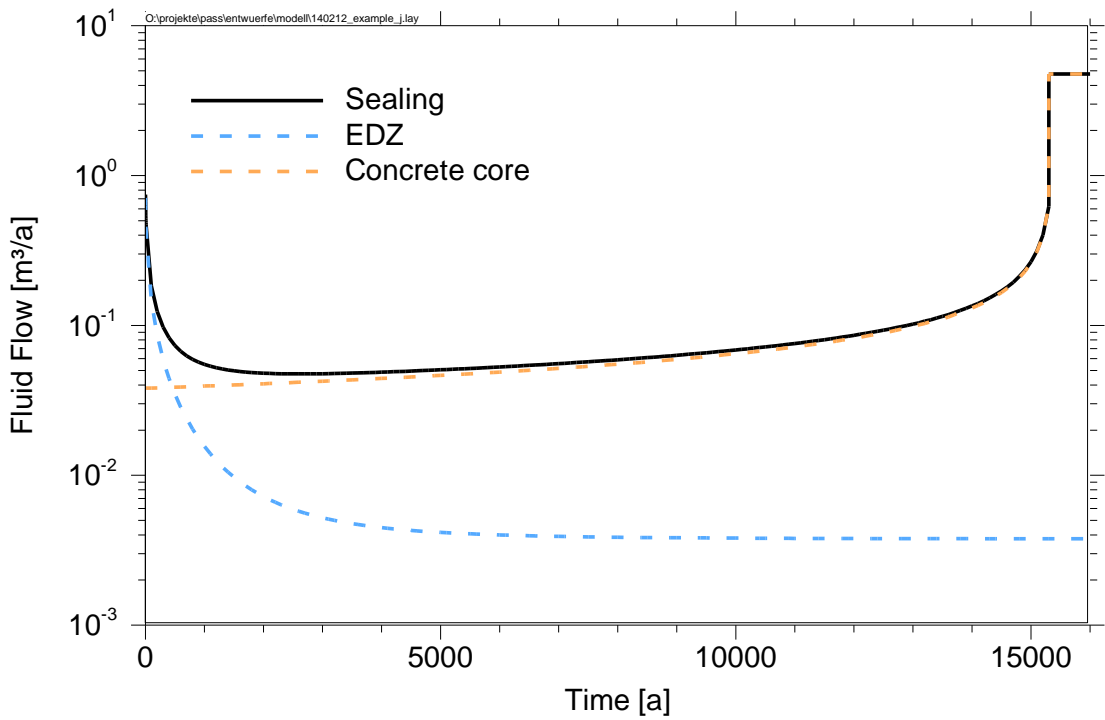

Fig. 8.2   Fluid flow through a sealing, its concrete core and the EDZ around the sealing versus time
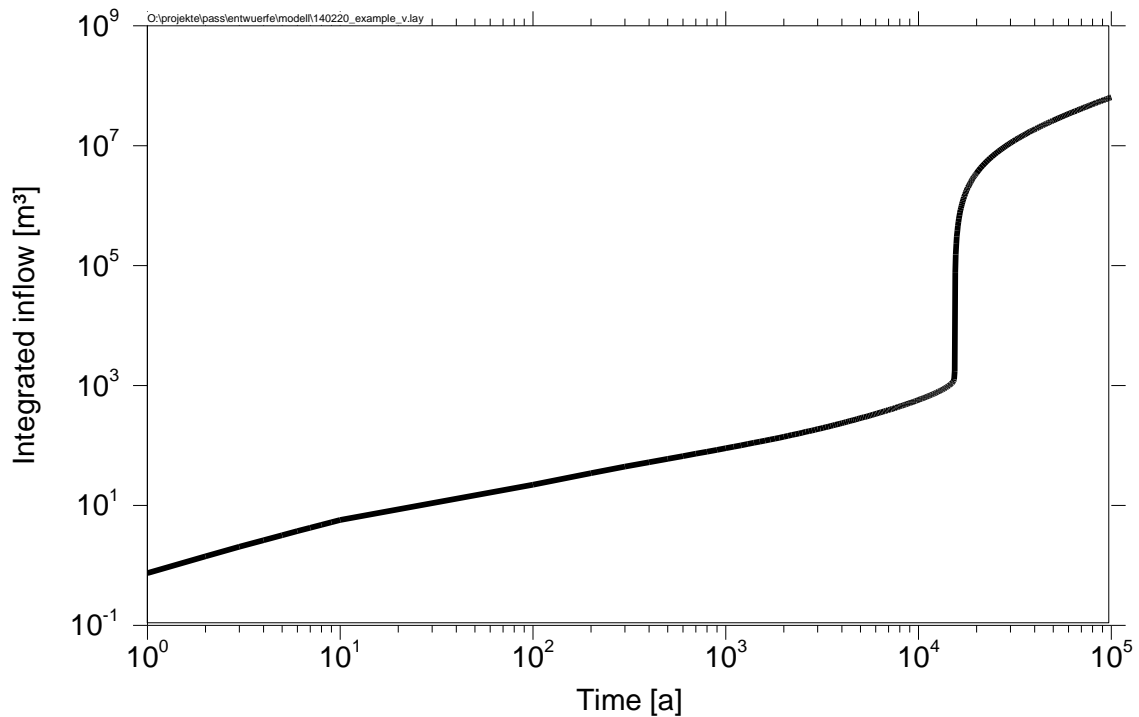
Fig. 8.3   Integrated inflow through sealing versus time

It has to be clearly noted that this is only an exemplary result which is highly sensitive to the input parameters listed above. Figure 8.4 shows some deterministic parameter variation where one parameter has been changed compared to the reference parameters in each calculation. The largest deviation compared to the reference case comes from the change of the sealing length. An increased sealing length by a factor of two results in a time needed to fully corrode the sealing which is increased by a factor of four.

A change of the corroded sealing permeability does not change the corrosion behaviour in a significant way before the sealing has been completely corroded. As long as there is a non-corroded part of the sealing, the sealing behaviour is dominated by this part. Changing the corrosion capacity does linearly change the time needed to fully corrode the sealing, but does not change integrated inflow curve for times before the sealing is fully corroded.

Changing the EDZ behaviour can significantly affect the amount of brine flowing through the sealing. This was tested by changing the extension of the EDZ into the host rock and the fitting parameter a resulting in a delay by a factor of five to close the EDZ. However the effect of both changes is completely overruled at the point in time when the sealing is fully degraded by salt cement corrosion.
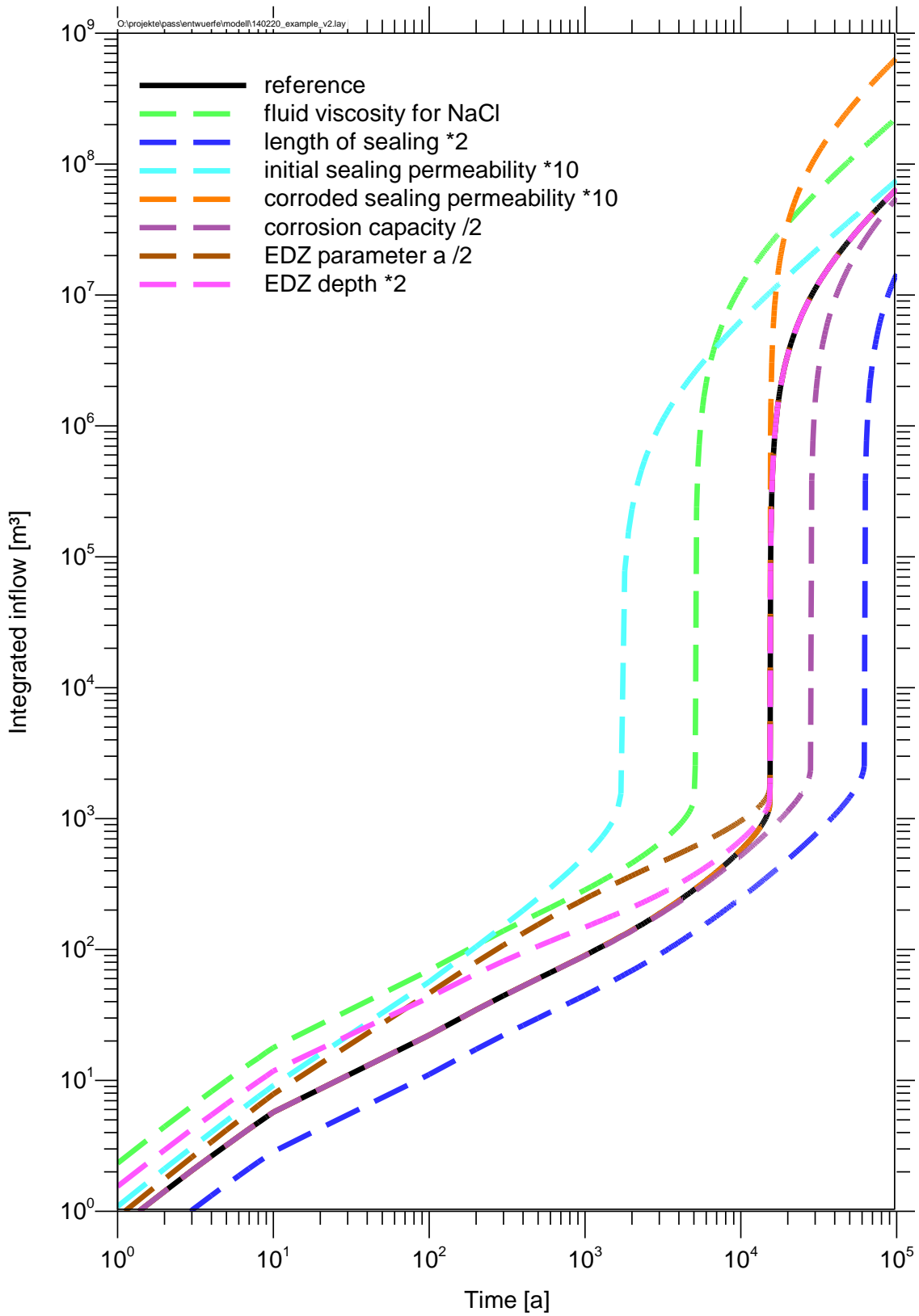
34

Fig. 8.4 Integrated inflow through sealing versus time for different parameter variations

9 Development of the LOPOS segment model

In order to perform integrated performance assessment including sensitivity analysis the mathematical models, described in chapters 6 and 7, have been implemented in the numerical code LOPOS, described in chapter 4. This was achieved by means of extending existing segment models for vertical and horizontal drifts and shafts to consider the effects of concrete corrosion and time dependent permeability of excavation damaged zones (EDZ). In a first approach, each of these processes where implemented separately on its own in order to investigate the effects independently and avoid undesired cross-interactions. Subsequently, both processes of concrete corrosion and time dependent EDZ were combined into a single extended segment model for backfilled drift and shaft mine structures.

In order to accommodate time dependent variance of the hydraulic conductivity of the segments, the LOPOS program code had to be further developed and adapted appropriately. To reflect the changing hydraulic behaviour of the EDZ, which is induced by dilatancy reduction and healing of micro-fractures due to increasing rock pressure, the EDZ-permeability had to be no longer treated as constant but to develop in time. The temporal evolution of the EDZ is described as a function of time using the empirical fitting function:

$$k^E = k_\infty + k_0 e^{\left(-a \cdot t^b\right)} \tag{9.1}$$

with

t	time in years,
k_0	initial permeability value at $t = t_0$,
k_∞	permeability value converging against after long times and
a, b	curve shape fitting parameters.

The numerical implementation of this function was achieved by using four input parameters (k_0, k_∞, a, b) and the internal model variable t_N, representing the simulation time of the current time step, and with it calculating the actual time dependent permeability k^E of the EDZ for each time step successively. The resulting permeability is transferred to a separate routine that calculates the total hydraulic resistances of the entire sealing from permeabilities and geometric dimensions of EDZ and concrete core as described more detailed in chapter 5.

The numerical implementation to represent the concrete corrosion is however considerable more complicated. This is owing to the fact, that the progression of the corrosion front is implicitly controlled by the amount of brine flowing through the sealing, which is on the other hand controlled by the changing permeability due to corrosion. In order to solve the coupled problem, an incremental approach has been chosen. A separate subroutine calculates the incremental change of permeability dependent of the current flow rate through the sealing, which is calculated within the segment model itself beforehand, for each time step. Subsequently the hydraulic resistance for the entire sealing is again calculated from the permeabilities as described in chapter 5 in another subroutine, herein before mentioned.

The corrosion model described below is based on the following assumptions:

- The geometry of the sealing is square and straight.
- The sealing may be surrounded by a temporally constant or variant, but homogeneous EDZ.
- The corrosion proceeds one-dimensionally.
- The reaction zone is narrow enough to be considered as a sharp front.
- The viscosity μ of the brine and the porosity ϕ of the material remain constant.
- The permeability k changes abruptly at the corrosion front (by ε powers of ten).

The current flow through the entire sealing is split into parts, which flow through the concrete sealing element and through the EDZ. The brine in the EDZ around the sealing body is neglected for corrosion. This means that only the brine inflow into the concrete sealing element is available for the corrosion process.

Referring to chapter 5, the hydraulic resistances of the three parts of interest are as follows:

$$R_C^S = \frac{\mu L_C}{A^S k_C^S}, \quad R_0^S = \frac{\mu (L - L_C)}{A^S k_0^S}, \quad R^E = \frac{\mu L}{A^E k^E} \,. \tag{9.2}$$

Here, the lower index C denotes the corroded part of the sealing, while the lower index 0 denotes the intact area. The upper index S refers to the sealing material, while the upper index E refers to the EDZ. The character A represents the correspondent flow areas, while L denotes the total length of the sealing and L_C the length of the corroded part.

The total hydraulic resistance R of the sealing comprises of the partial hydraulic resistances for the sealing core and the EDZ, which are in parallel connection:

$$\frac{1}{R} = \frac{1}{R^S} + \frac{1}{R^E} .$$ (9.3)

Here, only the resistance R^S of the sealing core is assumed to be affected by corrosion. The corroded part and the non-corroded part of the sealing are linked by serial connection, according to the relation

$$R^S = R_C^S + R_0^S .$$ (9.4)

The effective permeability can now be calculated from the hydraulic resistance by means of the following equation:

$$R^S = \frac{\mu L}{A^S k_{eff}^S} .$$ (9.5)

From equations 9.4 and 9.5 we derive

$$\frac{1}{k_{eff}^S} = \frac{1}{L} \left(\frac{L_C}{k_C^S} + \frac{L - L_C}{k_0^S} \right) .$$ (9.6)

The permeability increases in the reaction front by ε powers of ten, i.e. $k_C^S = 10^\varepsilon k_0^S$, which reduces equation 9.6 to

$$\frac{1}{k_{eff}^S} = \frac{1}{L k_0^S} \left(\frac{L_C}{10^\varepsilon} + L - L_C \right) ,$$ (9.7)

which subsequently results to

$$\frac{k_{eff}^S}{k_0^S} = \frac{1}{10^{-\varepsilon} \frac{L_C}{L} + 1 - \frac{L_C}{L}} = \frac{1}{1 - \frac{L_C}{L} \left(1 - 10^{-\varepsilon} \right)} .$$ (9.8)

The volumetric corrosion capacity $\kappa_{L,V}$ specifies, which volume (solid phase) can be disintegrated by a standard volume of solution. For the total degradation of 1 m³ intact sealing material a brine volume of $(1-\phi)/\kappa_{L,V}$ m³ is required. The brine volume V_l, which has flown into the sealing when the corrosion front reaches the position L_C can be calculated to

$$V_l = \frac{1-\phi}{\kappa_{L,V}} A^S L_C + \phi A^S L_C = A^S L_C \left(\frac{1-\phi}{\kappa_{L,V}} + \phi \right).$$

(9.9)

The first term indicates the volume of brine that is needed for the degradation of the solid phase, the second results from the fact that the pore volume must be refilled with fresh solution. The volume of brine that is needed for the total corrosion of the sealing is therefore

$$V_L = V^S \left(\frac{1-\phi}{\kappa_{L,V}} + \phi \right),$$

(9.10)

where V^S equals the geometric volume of the sealing (concrete core only). By replacing the ratio L_C/L in equation 9.8 by V_l/V_L and in consideration of equation 9.10 finally follows

$$\frac{k_{eff}^S}{k_0^S} = \frac{1}{1 - \dfrac{V_l}{V^S} \dfrac{\kappa_{L,V}}{1-\phi-\phi\kappa_{L,V}} \left(1-10^{-\varepsilon}\right)}.$$

(9.11)

With the equation 9.11 the effective permeability of the corroding sealing can be calculated from the initial permeability k_0^S and the brine volume V_l streaming in with the aid of fixed parameters $\kappa_{L,V}$, ε, V^S and ϕ.

The mathematical models for corrosion induced permeability change of the concrete core along with time dependent behaviour of the surrounding EDZ are subsequently implemented into the numerical simulation code LOPOS. For this purpose, a new and extended segment type (segment notation 'ASQNX') has been developed, based on the previous, ordinary segment model for drifts and shafts with non-compressible backfill and excavation damaged rock zones (segment notation 'ASQNC').

An abbreviated description of the new segment type 'ASQNX' is given in the following:

Segment model 'ASQNX' ('HASQNX' for horizontal drifts, 'VASQNX' for vertical shafts) with non-compressible backfill and EDZ, considering

- pressure build-up during inflows by rise of water level,
- no gas storage,
- continuous flooding in the time interval *RBTY(2)* to *RBEY(25)*,
- continuously increasing pneumatic pressure from *RGY(12)* to *RGY(15)* for times between *RGY(16)* and *RGY(17)*.

Cross section:	rectangle
Porosity:	drift (shaft): locally, EDZ: locally
Permeability:	drift (shaft): locally time dependent, EDZ: locally time dependent
Convergence:	none
Discretization:	necessary (*IBEY (19) > 0*)
Exchange effects:	diffusion, dispersion, convection

Input parameters *IBEY*:

marker	meaning	value
1	number of input data *RBEY*	26
2	number of balanced flows *RUZY*	1
3	number of balanced flows *RUSY*	3
4	number of output data *RUDY*	30
5	number of time dependent output data *RBPY*	29
6	identifier for temperature sequence of backfill	
12	number of parallel drifts (shafts)	
13	number of parallel excavation damaged zones	
14	identifier for solubility limits	
15	identifier for sorption coefficients	
19	discretization: number of elements = 2**IBEY (19)*+1	

Input parameters *RBEY*:

marker	meaning	dimension
1	height of drift (shaft)	m
2	width of drift (shaft)	m
3	length of drift (shaft)	m
5	width (hight) of excavation damaged zone	m

6	length (width) of excavation damaged zone	m
8	brine volume for spontaneous intrusion	m^3
9	mass of sorbing material	kg
15	distance to reference level	m
17	permeability of drift	m^2
18	backfill porosity	-
19	initial permeability of excavation damaged zone	m^2
20	porosity of excavation damaged zone	-
21	final permeability of excavation damaged zone	m^2
22	EDZ fitting parameter a (temporal coefficient)	1/a
23	EDZ fitting parameter b (temporal exponent)	-
24	corrosion capacity kappa	m^3/m^3
26	permeability increase epsilon	-

Global data *RGY*:

marker	meaning	dimension
1	gravitational acceleration	m/s^2
2	universal gas constant	kJ/molK
3	average density of salt rock	kg/m^3
4	average density of fluid in mine	kg/m^3
5	dynamic viscosity of fluid in mine	Pa s
6	rock temperature on reference level	K
7	geothermal gradient	K/m
8	hydrostatic pressure on reference level	MPa
9	rock pressure on reference level	MPa
10	coefficient of expansion by concentration	m^3/mol
11	thermal expansion coefficient	1/K
12	atmospheric pressure	MPa
15	impressed air pressure	MPa
16	begin of pressure increase	a
17	end of pressure increase	a
25	stress exponent	-
66	diffusion coefficient in brine	m^2/s
67	diffusion activation energy	K
69	dispersion length in backfilled areas	m
70	convection speed in drifts and chambers	m/a

The numerical code LOPOS is accompanied by a graphical user interface called XENIA. The user interface XENIA is an essential part of the program package repo-TREND, which LOPOS is part of, and assists to compile input data for numerical models as well as to start and manage computational runs. Thus, it takes control of simulation runs by automatically generated script files and forwards them for computational processing to a specified cluster or workstation.

The input data and additional information of the simulation runs are stored in a relational database (PostgreSQL); each simulation run is uniquely assigned to a project or subproject. The use of (sub-)projects has been introduced as the highest classification level of the database for the systematic filing of the simulation runs. The following figure 9.1 represents a screenshot of the interface and provides an overview of the XENIA workspace and input masks for model parameters. A detailed description of procedures, views and configurations can be found in the program and user documentation for XENIA /REI 11/.
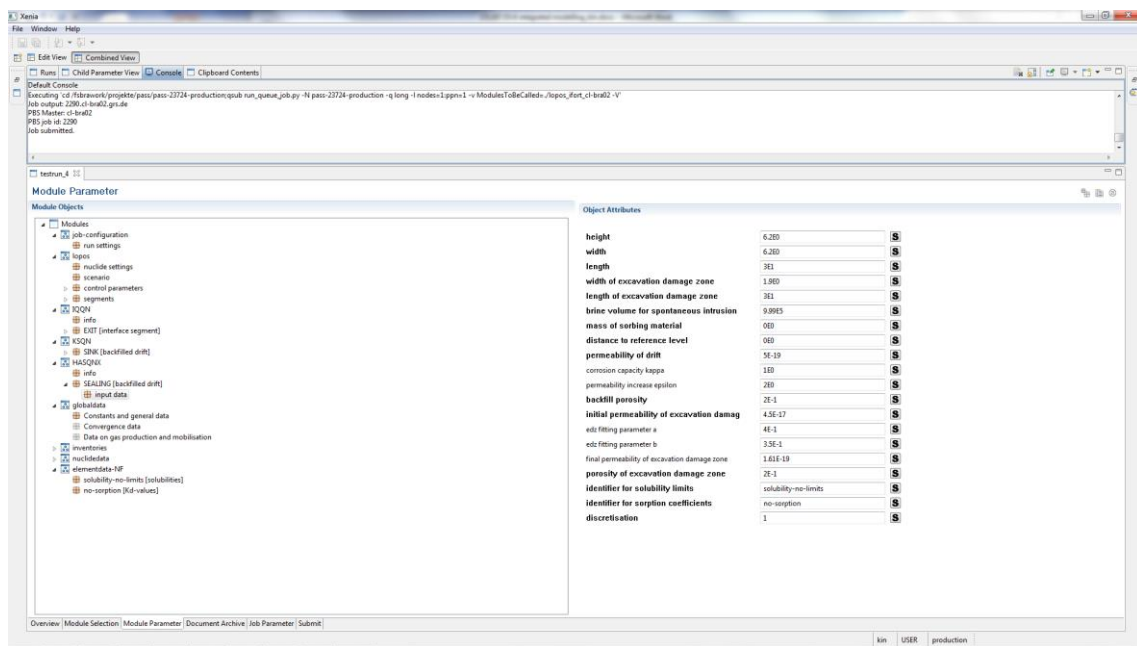
Fig. 9.1   Screenshot of XENIA interface for LOPOS model code

10   LOPOS model example calculation

The proper function of the newly developed LOPOS segment model 'ASQNX' is demonstrated in a test calculation of a single sealing exposed to constant brine pressure. The model results are compared to the quasi analytic solution of the same test case presented in the illustrative example calculation of chapter 8.

The input parameters for the test calculation parallel those of the illustrative example in chapter 8 and are given in table 10.1. Instead of analytical spreadsheet analysis the integrated performance assessment code LOPOS was used to calculate the brine outflow through the sealing element – including effects of time dependent EDZ evolution and corrosion of salt concrete as described in the chapter above.

Tab. 10.1   Model test calculation parameters

Parameter		Value
Length of the sealing	[m]	30
Height of the sealing	[m]	6.2
Width of the sealing	[m]	6.2
Hydraulic pressure at sealing	[MPa]	10
Dynamic viscosity of brine μ	[Pa s]	$5.3 \cdot 10^{-3}$
Porosity of salt concrete material ϕ	[-]	0.2
Initial permeability of salt concrete material k_0^S	[m^2]	$5 \cdot 10^{-19}$
Permeability increase ε	[-]	2
Corrosion capacity of the brine $\kappa_{L,V}$	[l/l]	1
Width of excavation damaged zone	[m]	1.9
EDZ initial permeability k_0	[m^2]	$4.5 \cdot 10^{-17}$
EDZ long-term permeability k_∞	[m^2]	$1.6 \cdot 10^{-19}$
EDZ fitting parameter a	[-]	0.4
EDZ fitting parameter b	[-]	0.35

The results of the test calculation are shown in figures 10.1 and 10.2. Figure 10.1 illustrates the fluid flow rate through the sealing while figure 10.2 shows the integrated outflow. The black solid line represents the entire sealing and red or blue lines account for the partial flows through the concrete core as well as the EDZ around the sealing.
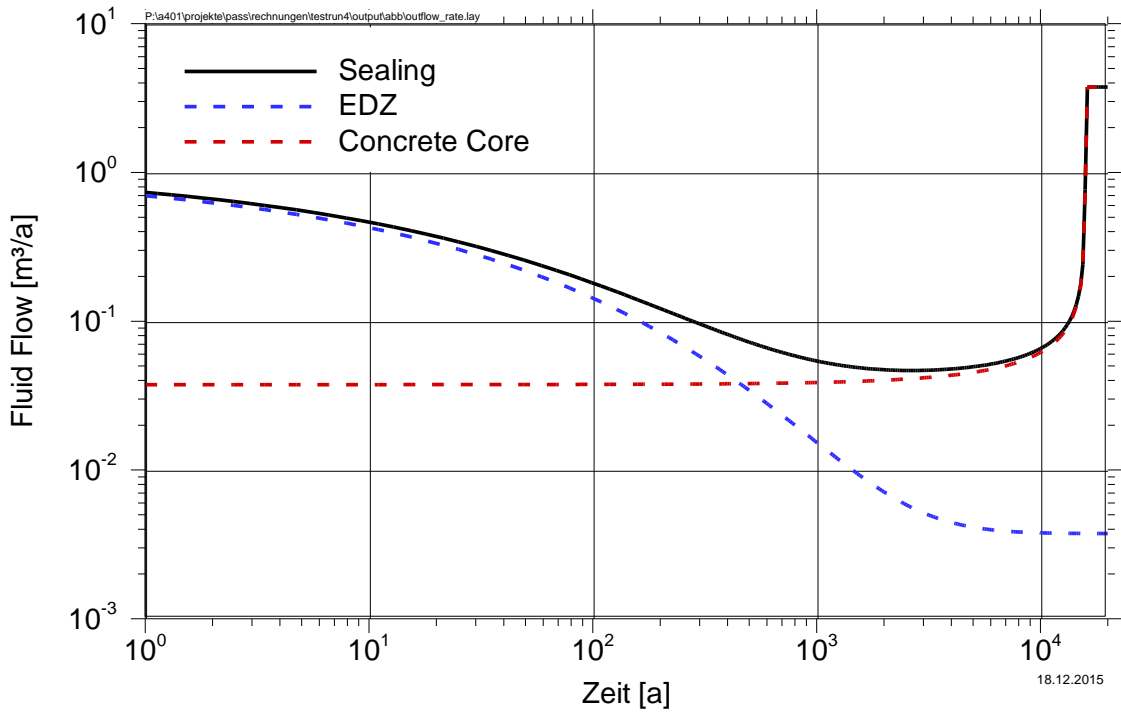
Fig. 10.1   Fluid flow through the sealing segment, its concrete core and the EDZ around the sealing versus time
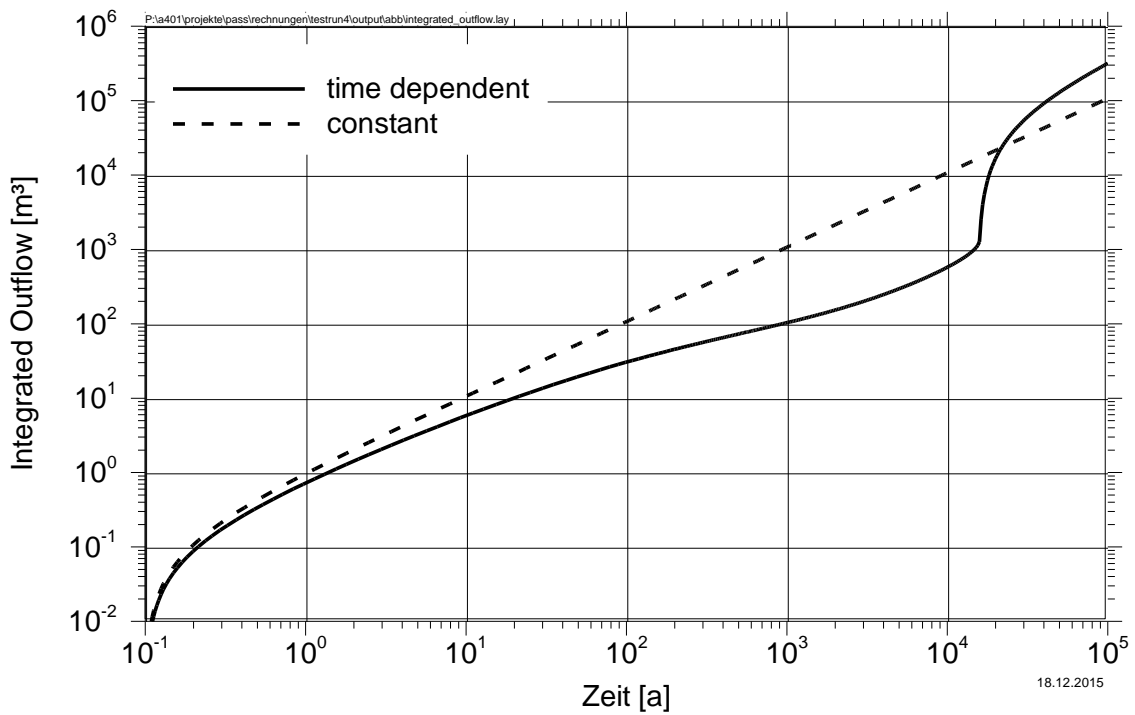
Fig. 10.2   Integrated outflow through sealing versus time

46

It can be noted that the resulting flow rates calculated with the numerical model are in good agreement with the results of the analytical spreadsheets presented in chapter 8. The time dependent fluid flow is dominated by the EDZ during the first few hundred years until healing processes reduce its hydraulic conductivity. The resistance of the concrete core dictates from thereon the behaviour, even long before the corrosion front breaks through. After about 15 000 years the corrosion front reaches the back end of the sealing, leading to an abrupt decrease of the total hydraulic resistance. From that time on also the integrated outflow rises rapidly, as can be seen from figure 10.2.

To evaluate the obtained results in comparison to the previous model concept of constant hydraulic behaviour of the sealing, some further interpretation of the pictured diagrams is useful. Looking at the temporal evolution of the fluid flow rate through the sealing it can be seen in figure 10.1, that due to EDZ closure it is reduced by about one order of magnitude already after about 500 years and remains on that low-level for more than the next 10 000 years. Only after the corrosion front breaks through at about 15 000 years, the flow rate exceeds initial values. From figure 10.2 we also realize, that the total amount of brine discharge from the sealing is significantly decreased to previous assumption of constant permeabilities for more than 20 000 years. At later times, the higher permeability of the corroded concrete takes effect. In case of actual repository layout and barrier design it has to be ensured, that long-term sealing elements (crushed salt) obtain their projected performance beforehand.

11 Simulations for the VSG shaft sealing concept

The following integrated performance assessment modelling refers to the shaft sealing concept developed within the scope of the Preliminary Safety Analysis for Gorleben (VSG) that was introduced in chapter 3. For this sealing concept, integrated performance assessment model calculations were performed for several scenarios. Previous model calculations yielded good results although neglecting effects of time dependent hydraulic properties as investigated within the DOPAS project /MUE 12a/. The aim of the new model calculations presented here is to compare previous model results with new results obtained with the extended LOPOS segment model described above.

The investigations are carried out with the computer code LOPOS of the program package RepoTREND, for which a version is used, that enables the consideration of depth dependent volume flows (LOPOS8).

The shaft sealing concept, which was developed within the framework of the Preliminary Safety Analysis for Gorleben, was already introduced in chapter 3 and illustrated in figure 3.1. The shaft sealing mainly consists of three sealing elements made of different materials, abutments and supplementary components. In figure 11.1 the segment structure of the shaft sealing created for the LOPOS model is shown schematically. The lengths of the individual components correspond to those of the shaft sealing concept illustrated in figure 3.1. The sacrificial layer was combined with the associated abutment. The infrastructure area performs as a sink segment representing the remaining repository and was taken into account only on the emplacement level of the mine.

The filter segment on the top of the first sealing element is not considered in the LOPOS-calculations as effective flow segment. Rather, this segment is used to ensure the pressure boundary condition at the upper edge of the first sealing element, that is, at 364 m model depth, a constant external pressure of 5.1 MPa due to the overlaying hydrostatic head.
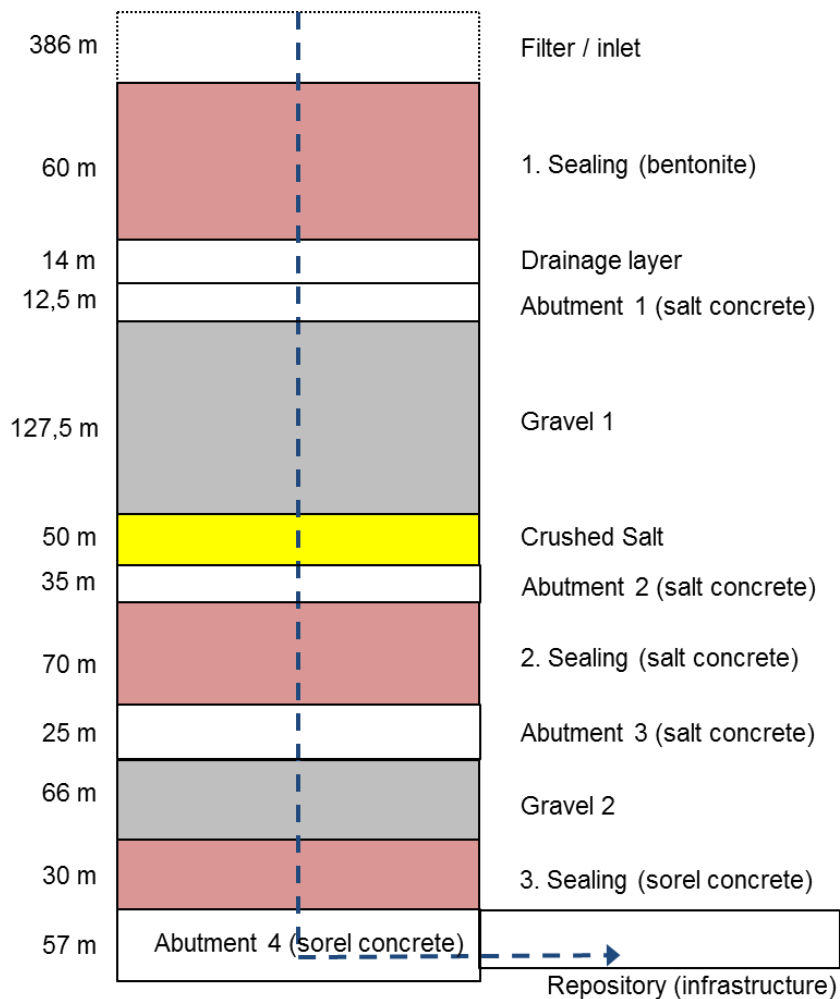
Fig. 11.1 Sketch of model segment structure for the shaft sealing concept including values for segment lengths

The initial saturation of the elements (0 = no solution in the segment; 1 = fully saturated) was considered in accordance with the technical specifications. The specified saturation refers to the initial gross pore volume. The total amount of solution in the shaft system is about 1700 m^3 at the beginning. In the model calculations with LOPOS this amount of trapped solution is taken into account in such a manner, that their volume is subtracted from the initial pore volume.

The starting date t=0 of the calculation refers to the completion date of the long-term sealing element. To simplify the calculation, it is assumed that the beginning of the brine inflow from the overburden (pressure build-up on the bentonite sealing element) corresponds to the time t=0 of the LOPOS model.

Tab. 11.1   Model parameters for the components of the shaft sealing

Functional component	length [m]	cross section [m²]	permeability [m²]	porosity	Initial saturation
Filter / inlet (sand/gravel)	436	5 x 5	$1 \cdot 10^{-12}$	30%	1
1. sealing element (bentonite)	60	8 x 7.31	$1 \cdot 10^{-17}$	27%	0.45
Drainage layer (gravel)	14	7 x 6.53	$1 \cdot 10^{-12}$	25%	0.6
Abutment 1 (salt concrete)	12,5	7 x 6.53	$1 \cdot 10^{-12}$	10%	0.85
Reservoir 1 (gravel)	127,5	7 x 6.53	$1 \cdot 10^{-9}$	23%	0.065
Long term sealing (crushed salt)	50	7 x 6.53	According PPR	**)10%	0.29
Abutment 2 (salt concrete)	35	8 x 7.65	$2 \cdot 10^{-15}$	10%	0.85
2. sealing element (salt concrete)	70	8 x 7.65	$7 \cdot 10^{-19}$	10%	0.85
Abutment 3 (salt concrete)	25	8 x 7.65	$2 \cdot 10^{-15}$	10%	0.85
Reservoir 2 (gravel)	66	7 x 6.53	$1 \cdot 10^{-9}$	38%	0.065
3. sealing element (sorel concrete)	30	8 x 8.36	$5 \cdot 10^{-17}$	16%	0.8
Abutment 4 (sorel concrete)	57	8 x 8.36	$5 \cdot 10^{-17}$	16%	0.8
Infrastructure (horizontal)	1000	*)57 x 10	$1 \cdot 10^{-14}$	40%	0

*) height equal to abutment 4 because of horizontal connection
**) initial value, conservatively treated as constant in the calculations

The length of the inlet segment is derived from a length of 386 m above the first sealing element plus 50 m on top by the assumed sea-level rise. The permeability of the long-term sealing was calculated according to a specified permeability-porosity relationship (PPR) for crushed salt to k=$1.3 \cdot 10^{-15}$ m² and is conservatively kept constant over time. The permeabilities of concrete sealing elements are treated as constants in the first instance. Those are afterwards being compared with the new model results considering time dependent permeabilities of concrete material as well as excavation damaged zones. Additional model parameters are given in Table 11.1.

In the following figures 11.2 to 11.6 the modelling results for the previous test case of unchanged permeabilities (referred to as 'srun2' – shaft simulation run #2) are presented. Figure 11.2 and 11.3 depict the volumes in selected shaft segments; in figure 11.2 for the upper segments and in figure 11.3 for the lower segments. In figures 11.4 and 11.5 the hydraulic pressure evolutions for the same segments are displayed. Figure

11.6 shows the cumulated brine inflow into the infrastructure area, which represents the adjacent repository.
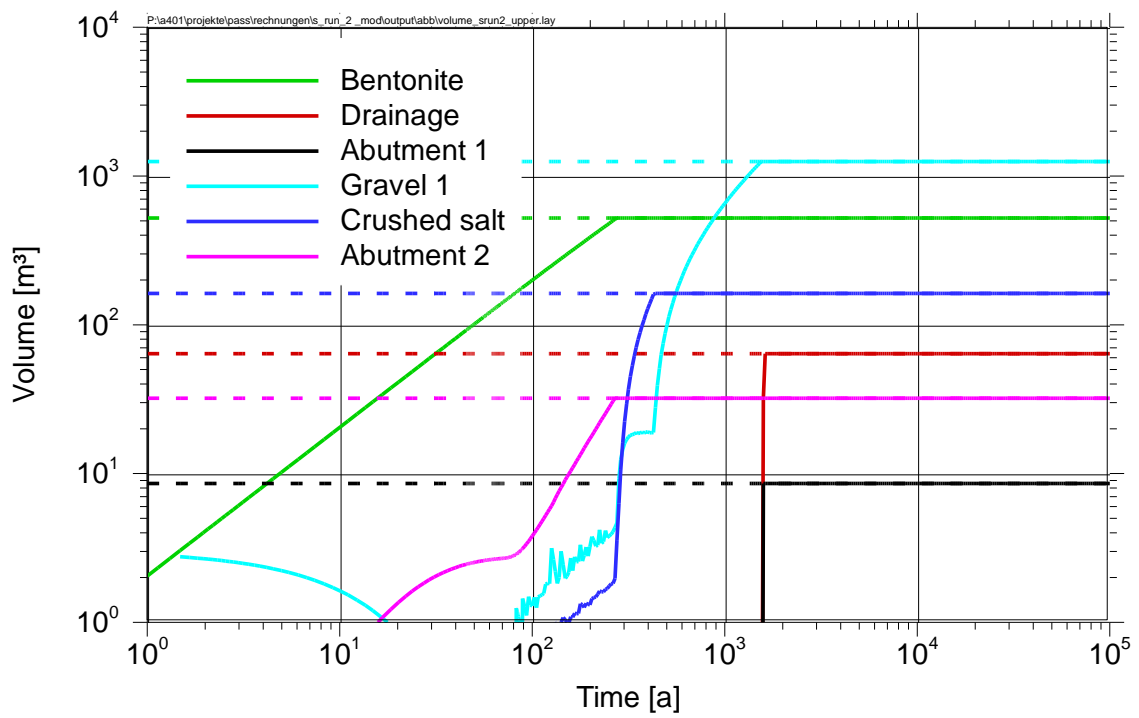
Fig. 11.2   Brine volumes of sealing elements versus time; srun2, upper segments
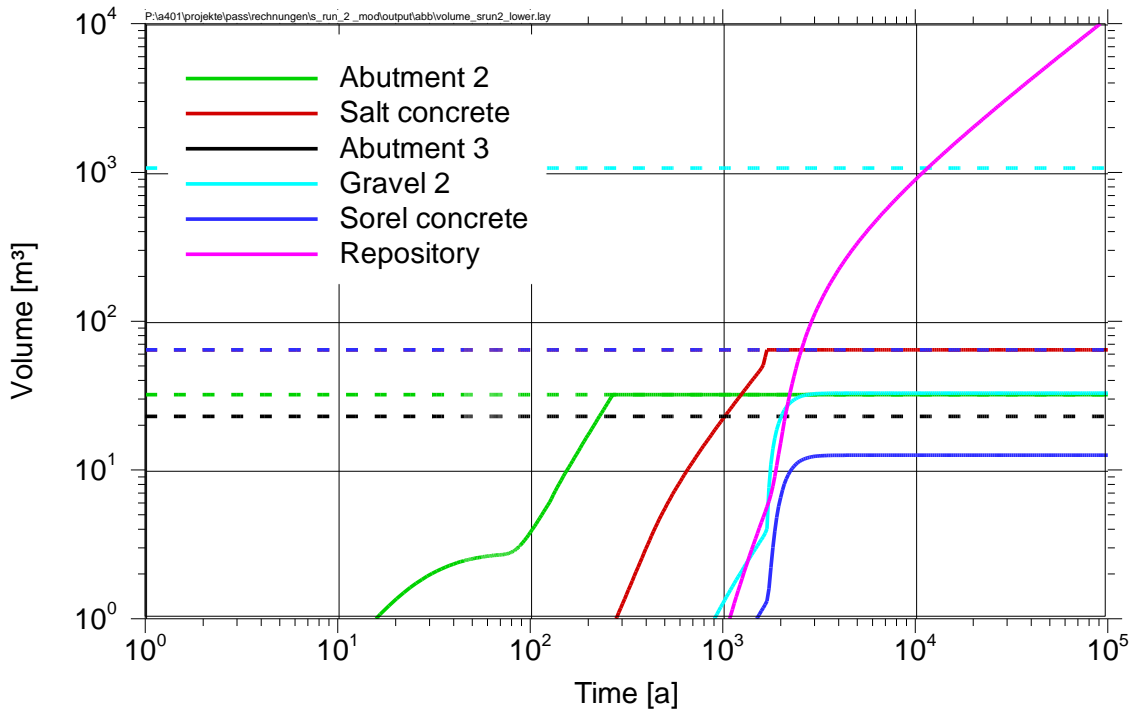
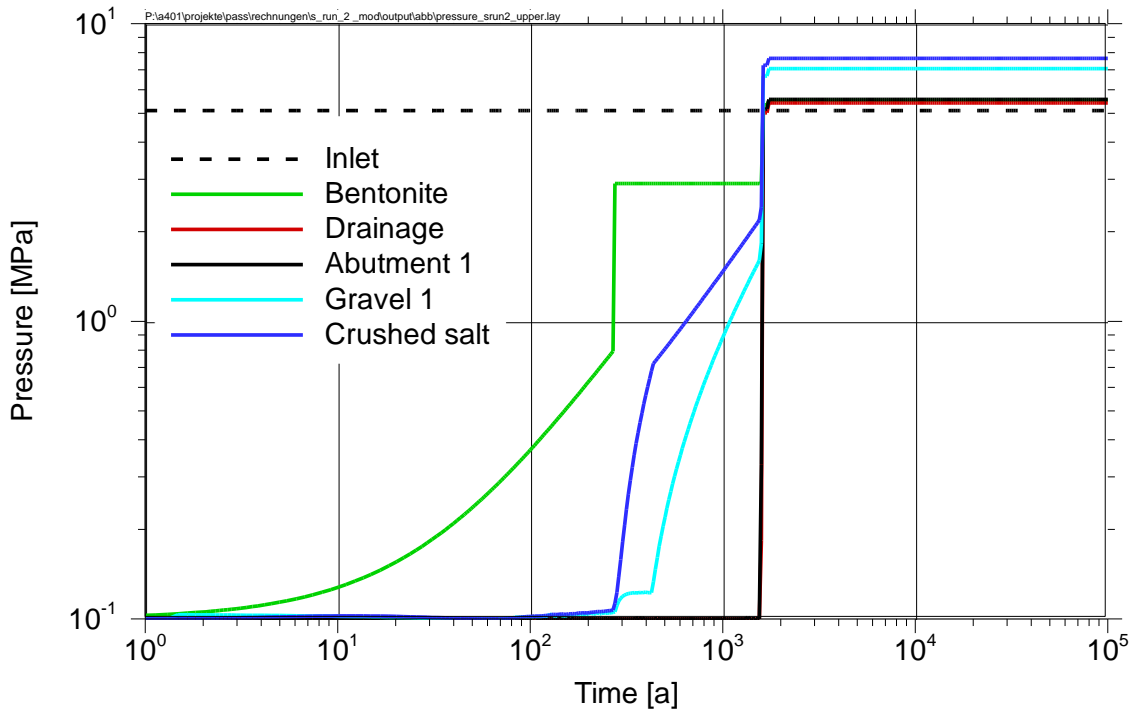**Fig. 11.3**   Brine volumes of sealing elements versus time; srun2, lower segments
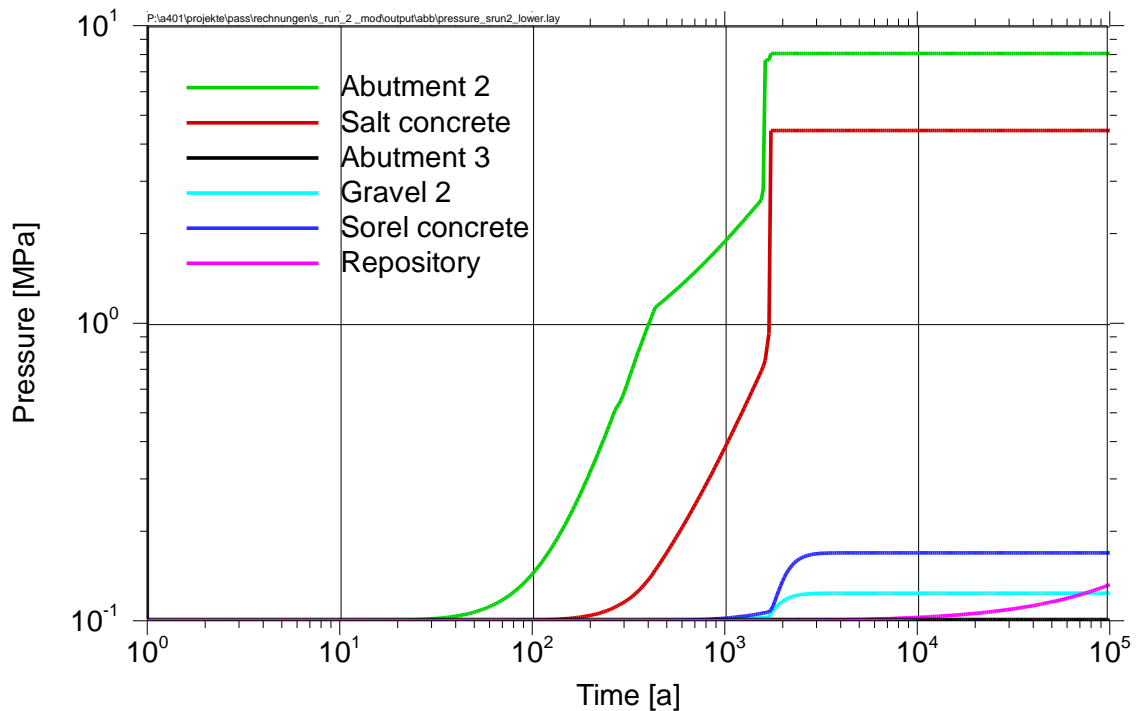

Fig. 11.4   Pressure evolution; srun2, upper segments

Fig. 11.5   Pressure evolution; srun2, lower segments

At the beginning of the calculation, all segments are filled with brine according to their initial saturation, see Table 11.1. This is represented in the model by an appropriately scaled pore volume. The inflow from the overburden into the shaft sealing coincides in the model with the inflow into the first sealing element of bentonite. As can be seen from figure 11.2, the pore space of the first sealing element is fully saturated after about 280 years. The intruding brine progresses further into the underlying components of the sealing system. After 280 years, the pore spaces of the abutment 2 and after 440 years those of the long-term sealing are saturated with brine. In quick succession after 1600 to 1740 years the pores in the gravel reservoir, the abutment 1 and the drainage layer are also fully saturated. In consequence, the water column piles up on top of the second sealing element (salt concrete), which exhibits the lowest hydraulic conductivity of all components.

Seeping brine from the salt concrete sealing element percolates through the abutment 3 directly into the second gravel column; the abutment 3 is hence filled only by very small amounts of brine. The second gravel column and the subsequent sorel concrete sealing element reach a steady state after approximately 3000 years; the inflowing brine will be forwarded directly to the infrastructure area. Over a 100 000 years model time about 10 000 m³ brine are passing through the entire shaft sealing and reach the infrastructure segment, which represents the repository area, cp. figure 11.6.
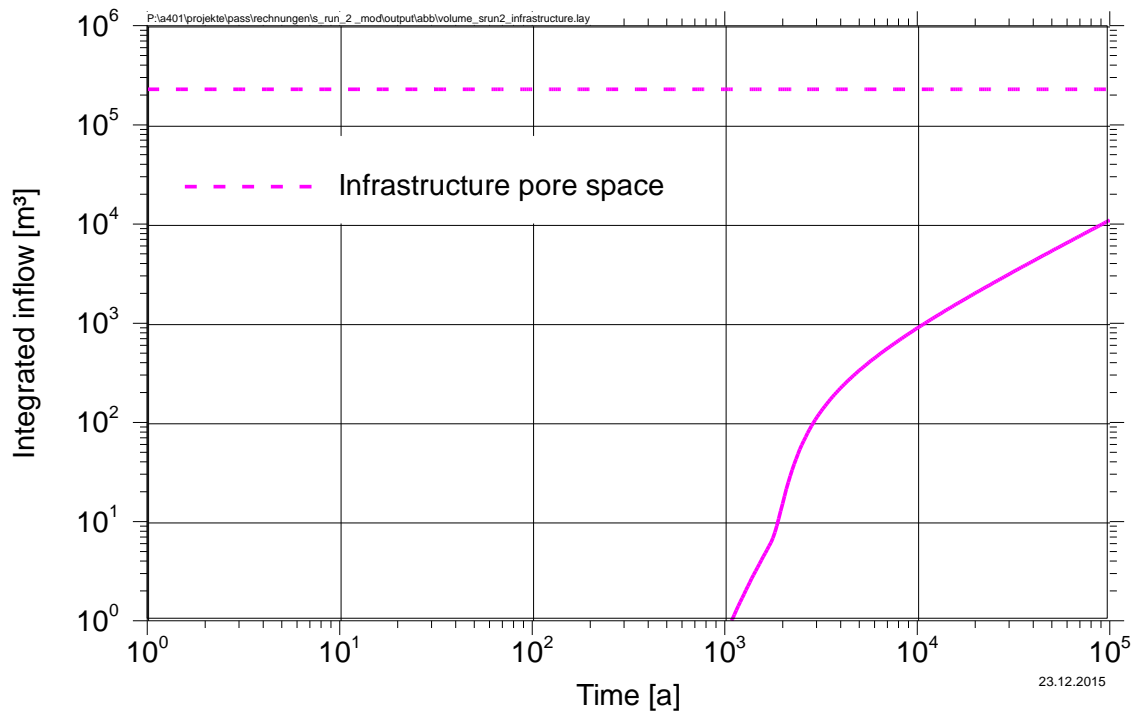
Fig. 11.6   Integrated inflow through sealing into repository versus time; srun2

The pressure at the top of the uppermost sealing element (bentonite) is constant and amounts to 5.1 MPa accordingly 436 m water column, cp. figure 11.4. After the date of full saturation of the pore space in the drainage layer and the gravel column (1600 years) the pressure in the bentonite increases to 5.35 MPa. There and in every other component above the salt concrete sealing the maximum values are reached in the period after 1740 years, when the sealing element of salt concrete is saturated with inflowing brine. In all components underneath the salt concrete sealing element the pressures remain near atmospheric pressure and below 0.2 MPa throughout the whole model time.

In the following, the results of the advanced test simulations 'srun2a' (shaft simulation run #2 with excavation damaged zones only), 'srun2c' (with concrete corrosion only) and 'srun2x' (fully extended with EDZ and corrosion combined) are being presented. These new test cases refer to the ELSA shaft sealing concept presented above with the extension of time dependent EDZ and/or concrete corrosion for the second and third sealing element, namely the salt concrete and MgO-based concrete sealings. Accordingly, the newly developed segment model VASQNX is applied to represent the 2nd and 3rd sealing elements. The parameters for EDZ evolution and concrete corrosion were selected consistent with the exemplary values given in chapters 6 and 7 and represent an Mg-content of the brine of about 10 % of that of an IP-21 solution. Re-

55

maining parameters were left unchanged compared to the previous simulation 'srun2', the reference case. A compilation of added and/or altered test case parameters is given in table 11.2.

Tab. 11.2 Model parameters for advanced test case simulations

Added/altered parameter	Model test case			
	srun2	srun2a	srun2c	srun2x
Initial permeability of salt concrete material k_0^S [m²]	$7 \cdot 10^{-19}$	$7 \cdot 10^{-19}$	$7 \cdot 10^{-19}$	$7 \cdot 10^{-19}$
Permeability increase ε of salt concrete [-]	-	-	4	4
Corrosion capacity of the brine (salt concrete) $\kappa_{L,V}$ [l/l]	-	-	0.225	0.225
Initial permeability of sorel concrete material k_0^S [m²]	$5 \cdot 10^{-17}$	$5 \cdot 10^{-17}$	$5 \cdot 10^{-17}$	$5 \cdot 10^{-17}$
Permeability increase ε of sorel concrete [-]	-	-	2	2
Corrosion capacity of the brine (sorel concrete) $\kappa_{L,V}$ [l/l]	-	-	0.07	0.07
Cross section of excavation damaged zones [m²]	-	2.8	-	2.8
EDZ initial permeability k_0 [m²]	-	$4.5 \cdot 10^{-17}$	-	$4.5 \cdot 10^{-17}$
EDZ long-term permeability k_∞ [m²]	-	$1.6 \cdot 10^{-19}$	-	$1.6 \cdot 10^{-19}$
EDZ fitting parameter a [1/a]	-	0.4	-	0.4
EDZ fitting parameter b [-]	-	0.35	-	0.35

The results of the new test case simulations 'srun2a', 'srun2c' and 'srun2x' are presented in the following figures 11.7 to 11.11. Figures 11.7, 11.8 and 11.9 depict the brine volumes of the lower sealing segments for each calculation run compared to the reference test case 'srun2' (dashed lines).

Figure 11.7 represents the results for considering time dependent EDZ around the second and third sealing element. It can be observed that the resulting brine volumes are only slightly affected by EDZ closure and consequences appear nearly negligible after a period of about 2000 years.

Figure 11.8 depicts the resulting brine volumes in case of corroding concrete sealing elements. Here, it can be observed that the consequences of concrete corrosion only

at late times (after about 10 000 years) gain in importance. The backup gravel reservoir between the two concrete sealing elements is filled up rather quickly after full corrosion of the upper salt concrete, leading to an increased brine outflow from the lowest sealing segment into the infrastructure area. In consequence, the total amount of brine flown into the repository after the simulation period of 100 000 years has more than doubled if corrosion is being taken into account.

A combined consideration of time dependent EDZ and corrosion at the same time is shown in figure 11.9, confirming the results discussed before.
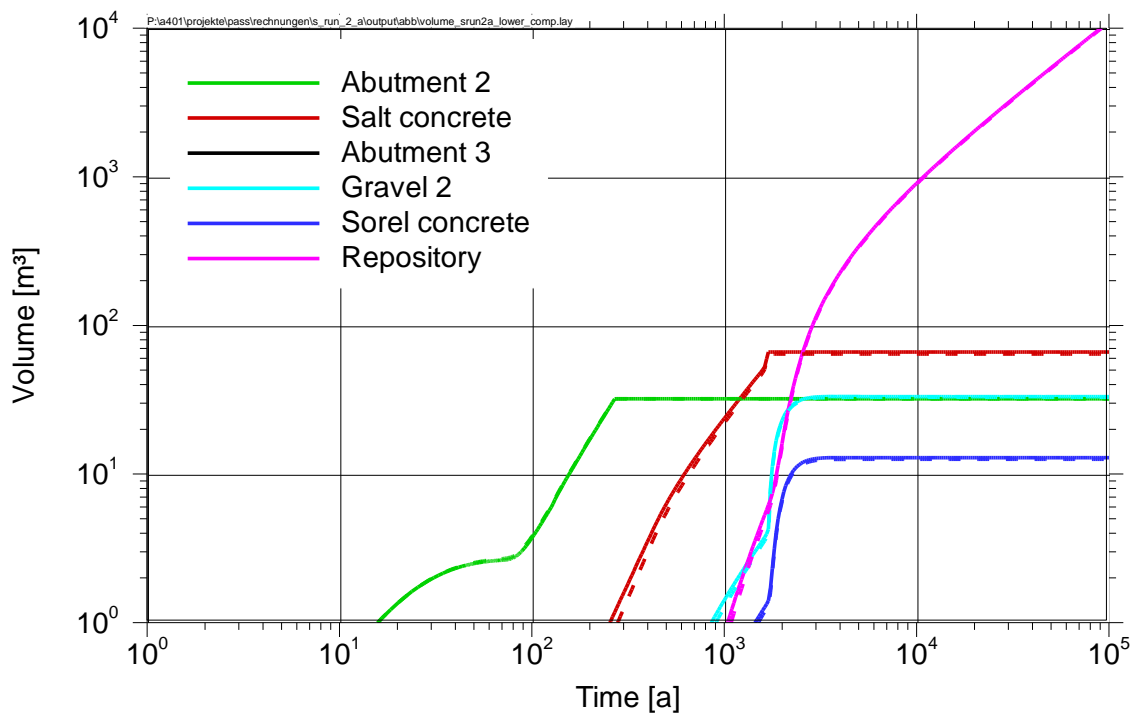
Fig. 11.7   Brine volumes of lower sealing elements over time; srun2a vs. srun2 (dashed)
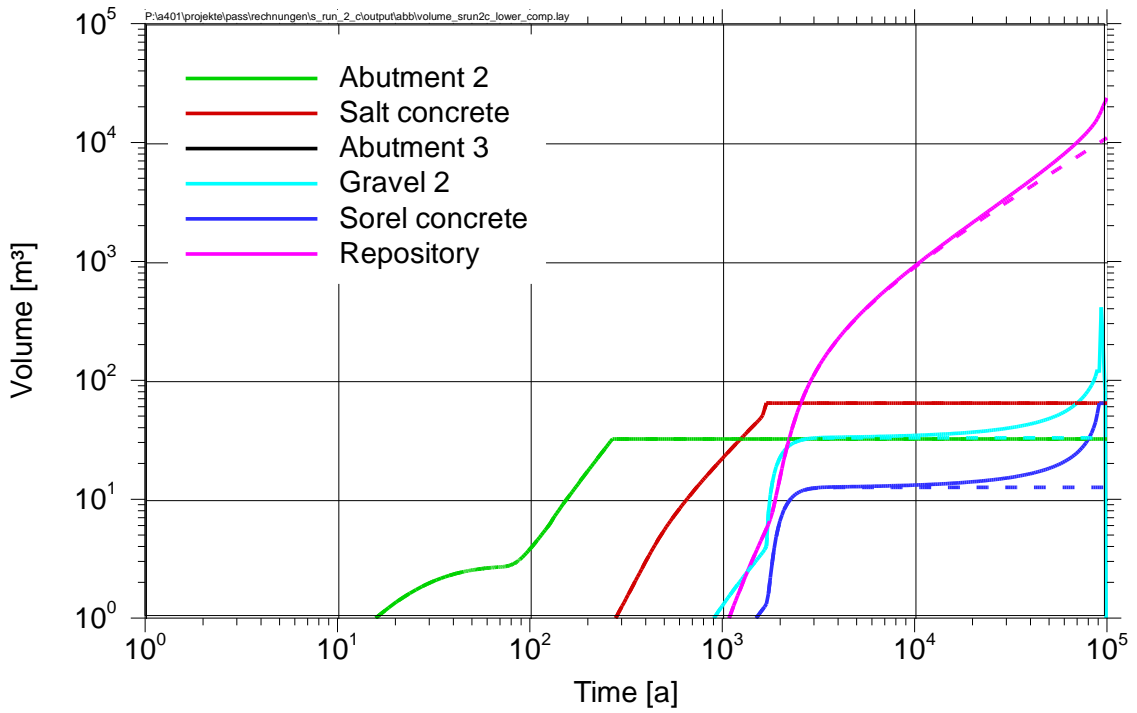
Fig. 11.8 Brine volumes of lower sealing elements over time; srun2c vs. srun2 (dashed)
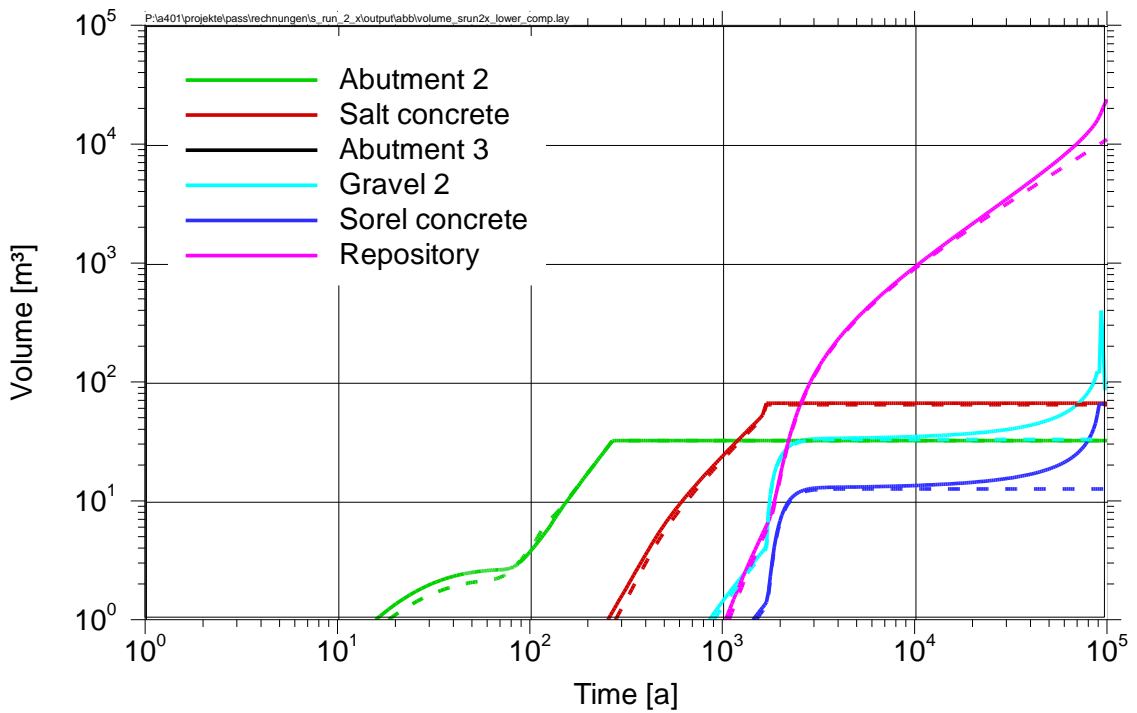
Fig. 11.9 Brine volumes of lower sealing elements over time; srun2x vs. srun2 (dashed)

To further illustrate the significance of the two processes EDZ-closure and concrete corrosion for an integrated performance assessment of real sealing systems in actual repository concepts an alternative presentation is chosen, clearly summarizing the results obtained. Therefore, figures 11.10 and 11.11 represent the direct comparison of the cumulated outflow from the sealing over time – equivalent to the integrated brine inflow into the repository area – for all four modelled test case scenarios in logarithmic and decadal scales. It can be noticed, that the consideration of EDZ-closure is having only slight effects at early times, almost completely vanishing in the long term (cp. srun2a vs. srun2). In contrast, the effects of concrete corrosion are negligible for early periods of time but exuberantly grow in importance in the long run.

Beyond that it can be observed that for long periods – from beginning till about 30 000 to 40 000 years – the brine outflow from the entire sealing system in the example presented here is virtually unaffected by EDZ-development and concrete corrosion. Hence, the conditions simulated provide sufficient time, that long-term sealing elements made of compacted crushed salt can fully develop their barrier effects long before concrete corrosion significantly reduces the effectiveness of the remaining sealing elements.
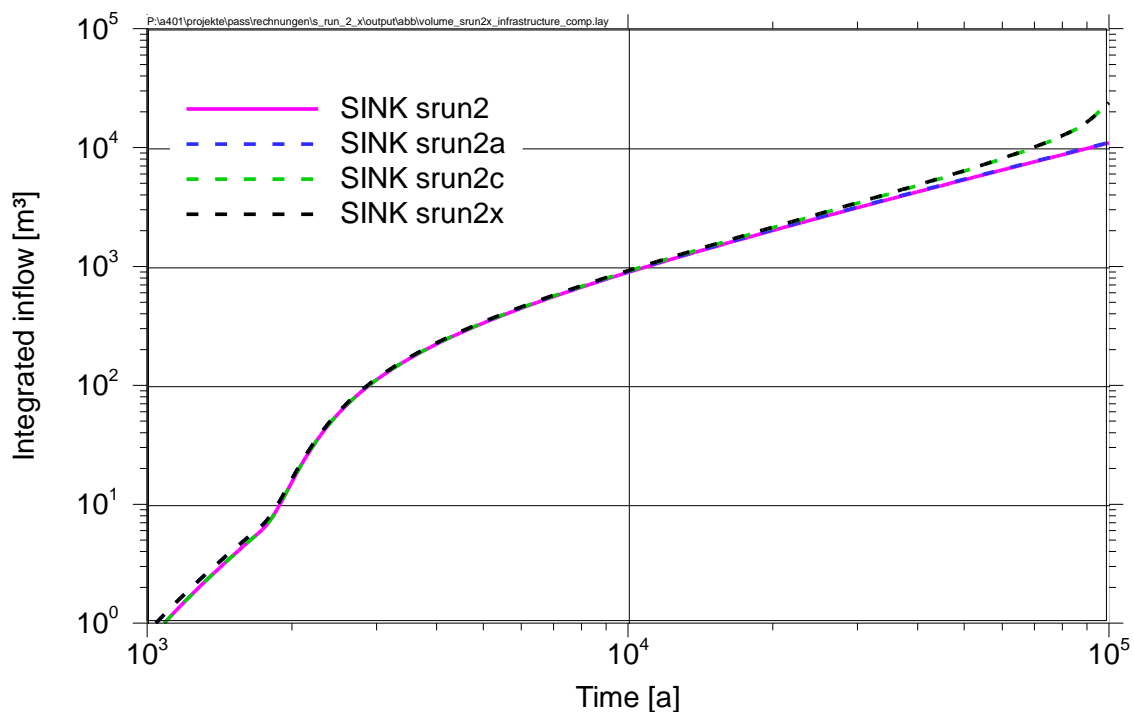
Fig. 11.10   Integrated inflow through sealing versus time – logarithmic scales; comparison of model cases
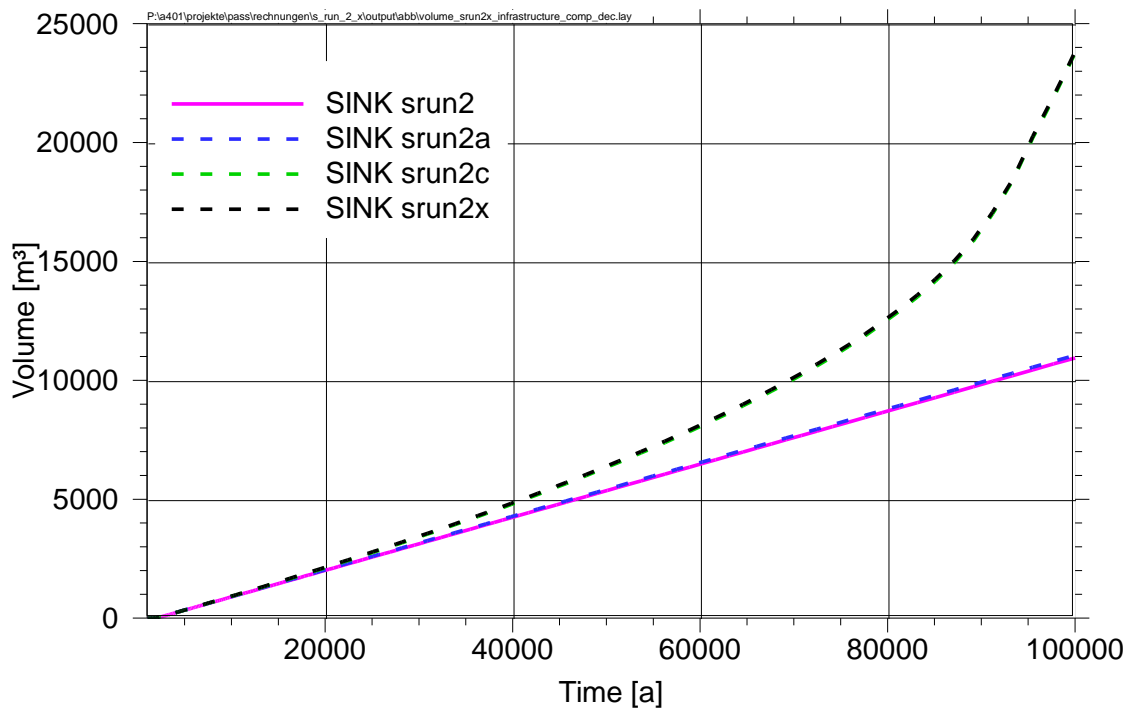
Fig. 11.11 Integrated inflow through sealing versus time – decadal scales; comparison of model cases

12   Probabilistic simulation tests

For the illustrative case presented in chapter 10, the influence of the parameter uncertainty was studied by a probabilistic Monte-Carlo simulation with 1.000 runs to test the probabilistic capabilities of the newly developed segment model. The bandwidth of the variation of the input parameters and the according probability density functions (PDF) are given in table 12.1.

Tab. 12.1   Probabilistic varied parameters

Parameter		lower limt	upper limit	probability density function
Length of the sealing	[m]	25	35	equal
Brine characteristic ξ		0	1	equal
Viscosity μ	[Pa s]	$2 \cdot 10^{-3}$	$6 \cdot 10^{-3}$	$\mu = (4\,\xi + 2)\,10^{-3}$
Porosity ϕ	[-]	0.1	0.3	equal
Initial permeability k_0^S	[m²]	$5 \cdot 10^{-20}$	$5 \cdot 10^{-18}$	log normal
Permeability increase factor	[-]	10^3	10^5	equal
Corrosion capacity $\kappa_{L,V}$	[l/l]	0.5	1.5	$\xi + 0.5$
EDZ initial permability k_0	[m²]	10^{-17}	10^{-14}	log normal
EDZ long-term perm. k_∞	[m²]	10^{-20}	10^{-17}	$k_0 / 1\,000$
EDZ fitting parameter a	[-]	0.15	0.6	normal

Those variables where an explicit function is given in the table instead of a PDF were varied dependent on another variable. The variation of the EDZ fitting parameter a was chosen in a way that the time needed for the resealing of the EDZ varies between 2.000 years and 80.000 years. Examples for the random parameter samples are shown in figure 12.1.
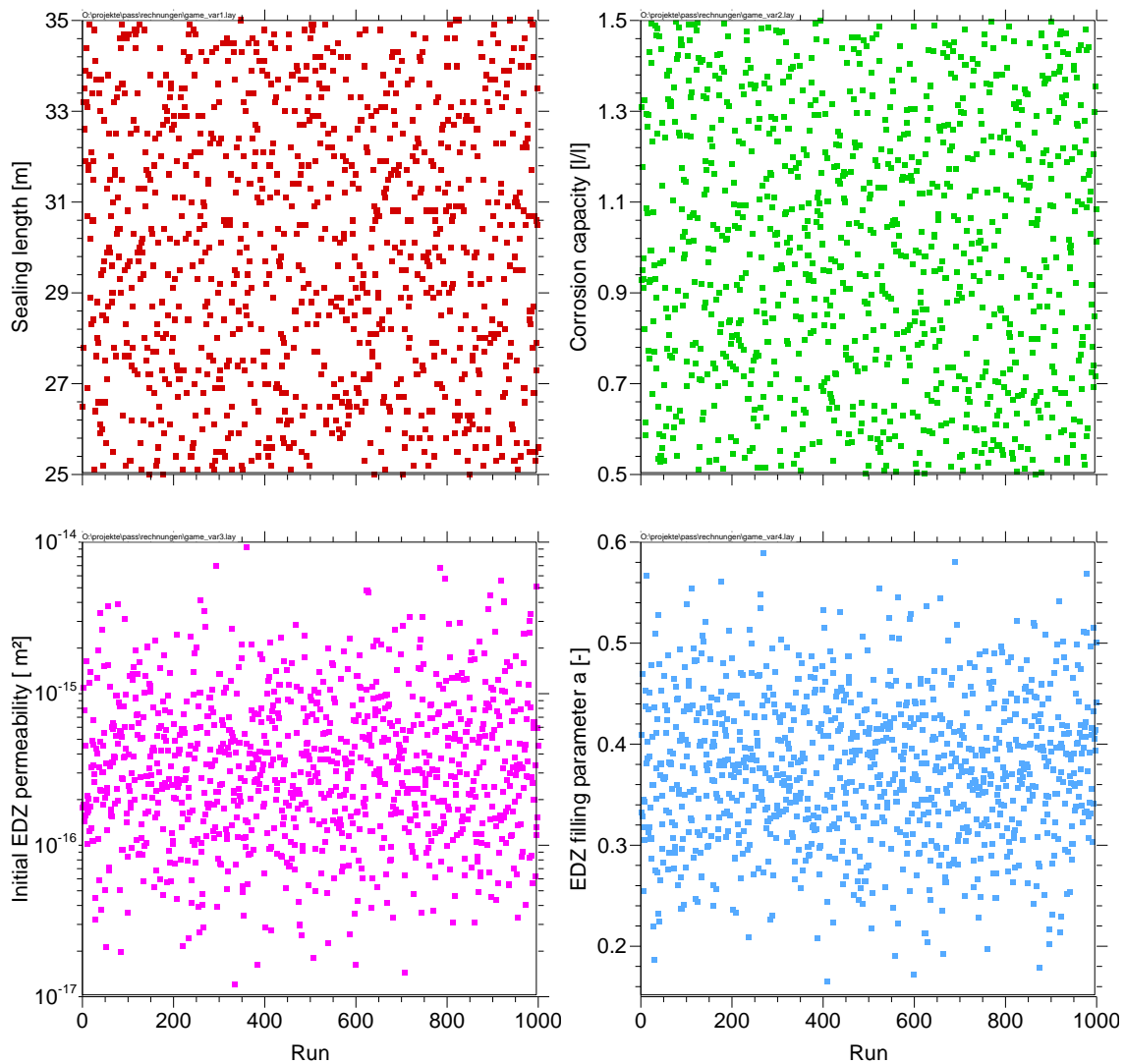
Fig. 12.1 Examples for the parameter distributions

As result of the probabilistic uncertainty analysis, figure 12.2 shows the cumulative brine flow through the sealing in the deterministic case together with the maximum, minimum, mean, median and the 5 and 95 percentiles of the probabilistic simulations. The result shows that the uncertainty of the result characterized by the bandwidth between the 5 and 95 percentiles is about two orders of magnitudes over most of the time. The uncertainty is even much higher during the phase of corrosion of the sealing material between some thousands and some tens of thousands years. A bit astonishing on the first glimpse might be that the deterministic case is lying at the lower end of the considered bandwidth. The reason for this is mainly that the EDZ permeability of the is at the lower end of the bandwidth of a log-normal PDF and therefore a rather unrealistic value from the view of the uncertainty analysis.
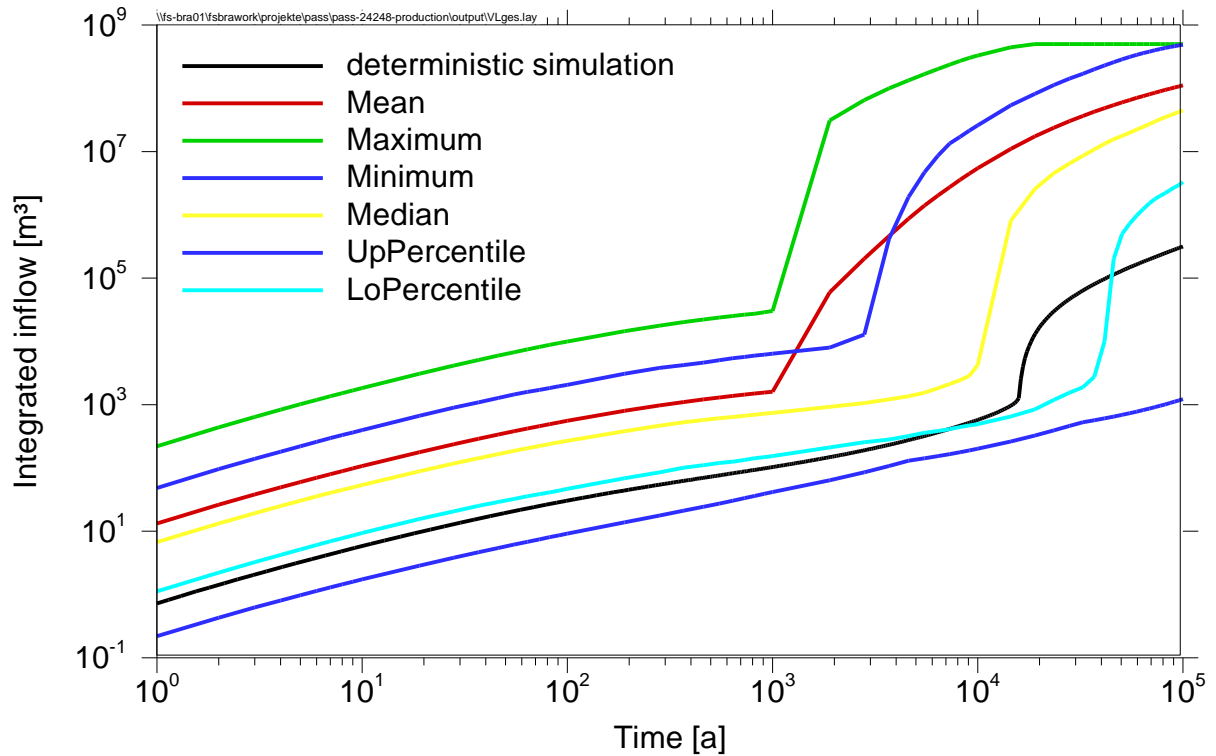
Fig. 12.2 Result of the probabilistic simulation compared to the deterministic simulation

A sensitivity analysis on the cumulative flow was performed on the probabilistic Monte Carlo simulation to determine the most important parameters influencing the simulation result. The following methods have been used for the evaluation: Standardised Regression Coefficients (SRC) Standardised Rank Regression Coefficients (SRRC), and Effective Algorithm for Computing Global Sensitivity Indices (EASI) (for the methods, see e.g. /RUE 10/). The result is shown in table 12.2 which shows the ranks of those parameters with a correlation coefficient greater 0.1 to the cumulative inflow at the end of the simulation run. The three parameters which are identified as sensitive for the cumulative flow at simulation end are all related to the corrosion process of the sealing material. The most sensitive parameter is more or less the permeability of the corroded material. This parameter is still ill defined and only known from process modelling due to the long experimental time needed to achieve the final state of the material in an experiment. Additional research might be needed to better define that parameter. However, additional parameters are sensitive if other times are regarded. For early times, the initial EDZ permeability is the most sensitive parameter (see figure 12.3).

Tab. 12.2 Ranks of the parameters in the sensitivity analysis

	SRC	SRRC	EASI
Length of the sealing			
Brine characteristic	3	3	
Porosity			
Permeability increase factor	1	1	1
EDZ fitting parameter			
Initial permeability	2	2	2
EDZ initial permability			
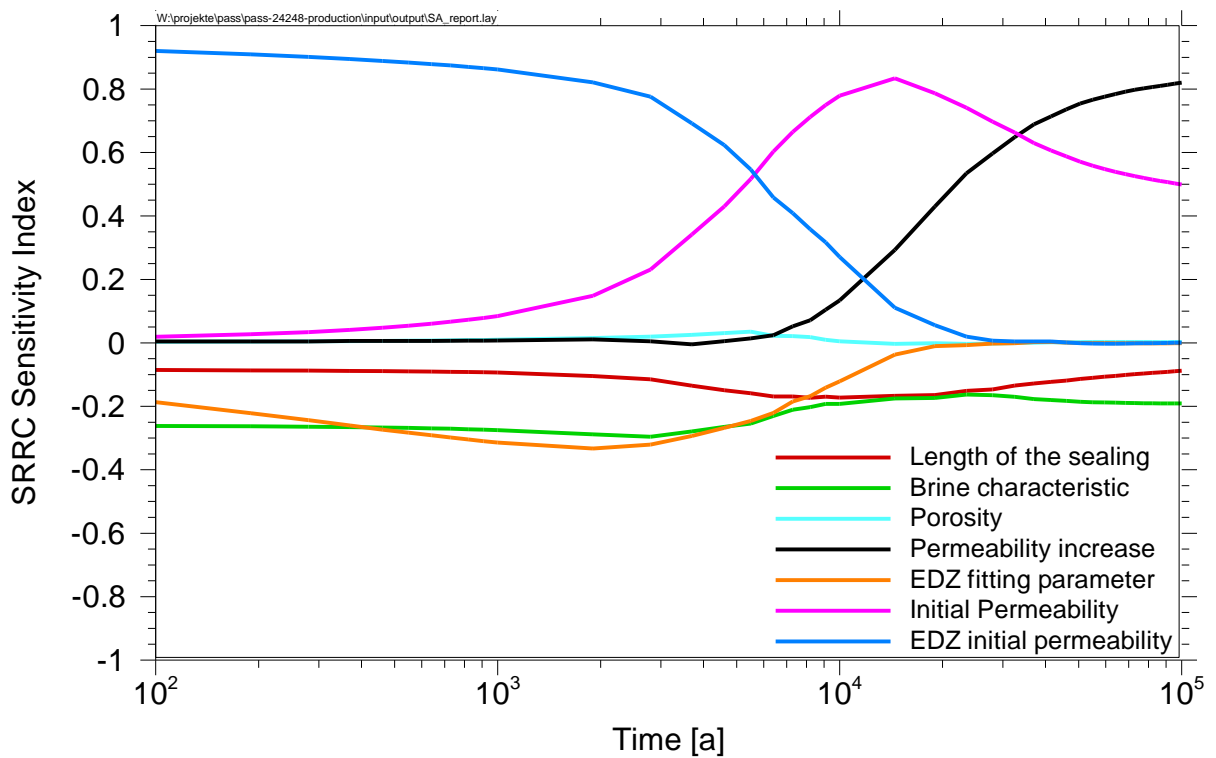
Fig. 12.3 Temporal evolution of the sensitivity indices for the PRCC method

13 Summary and conclusions

This report describes the work performed by GRS as part of the European project DOPAS. The aim of this work was to improve the way how geotechnical sealings are represented in integrated performance assessment models for radioactive waste repositories in salt.

A mathematical model was formulated that describes the long-term behaviour of a sealing system built from salt concrete. The average permeability of the sealing changes with time after its emplacement from various processes of which two were regarded in a conceptual model: first, the healing of the EDZ in the host rock around the sealing, and second, the corrosion of the salt concrete material resulting from brine attack. Empirical parameter model functions were defined for both processes to reflect the actual behaviour. The mathematical model was implemented in the integrated performance assessment code LOPOS which is used by GRS as near-field model for repositories in salt.

An example calculation was performed with realistic parameters showing how the permeability of the sealing decreases during the first 2 000 years due to the healing of the EDZ. Between 2 000 and 3 000 years, the calculated curves show a minimum permeability. After this time, the permeability increases again due to the progressing cement corrosion. A set of parameter variations and a probabilistic assessment was performed to determine the influence of parameter uncertainty. The example calculations show that the constitutive model is suitable to be used for future integrated performance assessment.

The new model was successfully applied to the ELSA shaft sealing concept. From the simulations it can be noticed that for periods from beginning of the post-closure phase until about 30 000 to 40 000 years, the brine outflow from the entire sealing system is virtually unaffected by EDZ-development and concrete corrosion. This is however, not such a great surprise, since the sealing system was designed accordingly from the beginning to not be largely affected by those effects.

Additional processes that might have to be considered in the future are cracks in the sealing material which allow for an advancing non-homogeneous corrosion of the sealing material along these pathways.

14 References

/BEC 02/ Becker, D.-A.; Buhmann, D.; Storck, R. et al.: Testing of Safety and Performance Indicators (SPIN). Final Report. European Commission, EUR 19965 EN, Brussels 2002.

/BEC 09/ Becker, D.-A.; Buhmann, D.; Mönig, J.; Noseck, U.; Rübel, A.; Spießl, S.: Endlager Morsleben, Sicherheitsanalyse für das verfüllte und verschlossene Endlager mit dem Programmpaket EMOS. Planfeststellungsverfahren zur Stillegung des Endlagers für radioaktive Abfälle Morsleben. Verfahrensunterlage P 278, 2009.

/BEH 04/ Bechtold, W.; Smailos, E.; Heusermann, S.; Bollingerfehr, W.; Bazargan Sabet, B.; Rothfuchs, T.; Kamelot, P.; Grupa, J.; Olivella, S.; Hansen, F.D.: Backfilling and sealing of underground repositories for radioactive waste in salt (Bambus II project). EUR 20621, European Commission, Luxembourg, 2004.

/BEU 12/ Beuth, T; Bracke, G.; Buhmann, D.; Dresbach, C.; Keller, S.; Krone, J.; Lommerzheim, A.; Mönig, J.; Mrugalla, S.; Rübel, A.; Wolf, J.: Szenarienentwicklung: Methodik und Anwendung. Abschlussbericht zum Arbeitspaket 8, Vorläufige Sicherheitsanalyse für den Standort Gorleben. GRS-284, Gesellschaft für Anlagen und Reaktorsicherheit (GRS) mbH, Köln, 2012.

/BIC 68/ Biczók, I. (1968): Betonkorrosion – Betonschutz. Bauverlag, Wiesbaden.

/BMU 10/ Federal Ministry for the Environment, Nature Conservation and Nuclear Safety: Safety Requirements Governing the Final Disposal of Heat-Generating Radioactive Waste. Version of Sept., 30. 2010. (http://www.bmu.de/files/english/pdf/application/pdf/sicherheitsanforderung en_endlagerung_en_bf.pdf)

/BOE 00/ Boese, B.; Hirsekorn, R.-P.; Storck, R.: Vergleich der Rechenprogramme LOPOS und MARNIE. Gesellschaft für Anlagen- und Reaktorsicherheit (GRS) mbH, GRS-169, Braunschweig 2000.

/BOL 11/   Bollingerfehr, W.; Filbert, W.; Lerch, C.; Tholen, M.: Endlagerkonzepte. Bericht zum Arbeitspaket 5. Vorläufige Sicherheitsanalyse für den Standort Gorleben. GRS-272, Gesellschaft für Anlagen- und Reaktorsicherheit, Köln, 2012.

/BOL 12/   Bollingerfehr, W.; Filbert, W.; Dörr, S.; Herold, P.; Lerch, C.; Burgwinkel, P.; Charlier, F.; Thomauske, B.; Bracke, G.; Kilger, R.: Endlagerauslegung und –optimierung. Bericht zum Arbeitspaket 6. Vorläufige Sicherheitsanalyse für den Standort Gorleben. GRS-281, Gesellschaft für Anlagen- und Reaktorsicherheit, Köln, 2012.

/BUH 10/   Buhmann, D., Mönig, J., Wolf, J., Keller, S., Mrugalla, S., Weber, J.R., Krone, J., Lommerzheim, A.: Nachweis und Bewertung des Isolationszustandes "Sicherer Einschluss". Teilbericht zum Projekt ISIBEL: „Überprüfung und Bewertung des Instrumentariums für eine sicherheitliche Bewertung von Endlagern für HAW" von DBE TECHNOLOGY GmbH, BGR und GRS, BMWi-FKZ 02E10065 und 02E10055. Peine, 2010.

/CZA 12/   Czaikowski, O.; Wieczorek, K.; Kröhn, K.-P.: Compaction of salt backfill – new experiments and numerical modelling. 7th Conference on the Mechanical Behavior of Salt: Saltmech7 Paris, 16–19 April 2012.

/GRS 06/   LOPOS AS6: Programmanpassungen und Verifikation für den Standort Asse. Projekt Langzeitsicherheit Asse – Transportmodellierung. Gemeinsames Projekt von NRG, Colenco und GRS. Gesellschaft für Anlagen- und Reaktorsicherheit (GRS) mbH, GRS-A-3338. November 2006.

/HER 05/   Herbert, H.-J.; Becker, D.; Hagemann, S.; Meyer, Th.; Noseck, U.; Rübel, A.; Mauke, R.; Wollrath, J.: Alteration of Non-Metallic Barriers and Evolution of Solution Chemistry in Germany. In: Engineered Barrier Systems (EBS) in the Context of the Entire Safety Case. Process Issues. NEA No. 6001, OECD, Paris, pp. 111–123, 2005.

/HEW 98/   Hewlett, P.C., ed.(1998): Lea's Chemistry of Cement and Concrete. Fourth Ed. Arnold, London.

/HIR 99/   Hirsekorn, R.-P.; Boese, B.; Buhmann, D.: LOPOS: Programm zur Berechnung der Schadstofffreisetzung aus netzwerkartigen Grubengebäuden. Gesellschaft für Anlagen- und Reaktorsicherheit (GRS) mbH, GRS-157, Braunschweig, Juni 1999.

/LAR 13/   Larue, J.; Baltes, B.; Fischer, H.; Frieling, G.; Kock, I.; Navarro, M.; Seher, H.: Radiologische Konsequenzenanalyse. Bericht zum Arbeitspaket 10. Vorläufige Sicherheitsanalyse für den Standort Gorleben. GRS-289, Gesellschaft für Anlagen- und Reaktorsicherheit, Köln, 2013.

/MOE 12/   Mönig, J.; Buhmann, D.; Rübel, A.; Wolf, J.; Baltes, B.; Fischer-Appelt, K.: Sicherheits- und Nachweiskonzept. Bericht zum Arbeitspaket 4. Vorläufige Sicherheitsanalyse für den Standort Gorleben. GRS-277, Gesellschaft für Anlagen- und Reaktorsicherheit, Köln, 2012.

/MUE 12a/ Müller-Hoeppe, N.; Engelhardt, H.-J.; Lerch, C.; Linkamp, M.; Buhmann, D.; Czaikowski, O.; Herbert, H.-J.; Wieczorek, K.; Xie, M.: Integrität geotechnischer Barrieren Teil 1: Vorbemessung. Bericht zum Arbeitspaket 9, Vorläufige Sicherheitsanalyse für den Standort Gorleben, GRS-287, Gesellschaft für Anlagen- und Reaktorsicherheit, Köln, 2012.

/MUE 12b/ Müller-Hoeppe, N.; Breustedt, M.; Wolf, J.; Czaikowski, O.; Wieczorek, K.: Integrität geotechnischer Barrieren Teil 2: Vertiefte Nachweisführung. Bericht zum Arbeitspaket 9, Vorläufige Sicherheitsanalyse für den Standort Gorleben, GRS-288, Gesellschaft für Anlagen- und Reaktorsicherheit, Köln, 2012.

/NOS 07/   Noseck, U.; Becker, D.; Rübel, A.; Meyer, Th.; Herbert, H.J.; Mauke, R.; Wollrath, J.: Treatment of drift seal performance in the long-term safety assessment for a repository in a salt formation. In: Engineered Barrier Systems (EBS) in the Safety Case: The Role of Modelling. OECD/NEA 6118, Issy-les-Moulineaux, 2007.

/OLI 08/   Olivella, S.; Alonso, E. E.: Gas flow through clay barriers, Geotechnique,58, No 3, 157–176, 2008.

/PEI 12/ Peiffer, F., McStocker, B., Gründler, D., Ewig, F., Thomauske, B., Havenith, A., Kettler, J.: Abfallspezifikation und Mengengerüst. Basis Ausstieg aus der Kernenergienutzung (Juli 2011). Bericht zum Arbeitspaket 3, Vorläufige Sicherheitsanalyse für den Standort Gorleben, GRS-278, Gesellschaft für Anlagen- und Reaktorsicherheit, Köln, 2011.

/REI 11/ Reiche, T., Becker, D., Buhmann, D., Lauke, T.: Anpassung des Programmpakets EMOS an moderne Softwareanforderungen, ADEMOS – Phase 1, GRS-A-Bericht 3623, Gesellschaft für Anlagen- und Reaktorsicherheit (GRS) mbH, Braunschweig, 2011.

/REI 16/ Reiche, T.: RepoTREND – Das Programmpaket zur integrierten Langzeitsicherheitsanalyse von Endlagersystemen, GRS-413, Gesellschaft für Anlagen- und Reaktorsicherheit (GRS) mbH, Braunschweig, 2016

/RUE 10/ Rübel, A.; Becker, D.-A.; Fein, E.; Ionescu, A.; Noseck, U.; Lauke, T.; Mönig, J.; Schneider, A.; Spießl, S.; Wolf, J.: Development of Performance Assessment Methodologies. GRS-259, Gesellschaft für Anlagen und Reaktorsicherheit (GRS) mbH, Braunschweig, 2010.

Figures

Tables